IEEE Access
Multidisciplinary | Rapid Review | Open Access Journal

Received September 24, 2018, accepted November 1, 2018, date of publication November 14, 2018,
date of current version December 18, 2018.

Digital Object Identifier 10.1109/ACCESS.2018.2881412

Selection Based List Detection With Approximate Matrix Inversion for Large-Scale MIMO Systems

TIANPEI CHEN[1] AND HARRY LEIB[2]
[1]Qualcomm, Inc., San Diego, CA 92121, USA
[2]Department of Electrical and Computer Engineering, McGill University, Montreal, QC H3A 0E9, Canada
Corresponding author: Harry Leib (harry.leib@mcgill.ca)

ABSTRACT Large-scale multiple-input multiple-output (LS-MIMO) technology constitutes a foundation for next generation wireless communication systems. Detection techniques are a key issue for practical applications of LS-MIMO. Selection-based list detection is an attractive approach for LS-MIMO systems because of its massively parallelizable nature. In this paper, we propose an improved selection-based list detection algorithm that exploits the channel hardening phenomenon, making it suitable for LS-MIMO. We start by introducing a low latency approximate inversion technique for large dimensional complex matrices, which can be used not only in selection-based list detection but also in many other LS-MIMO detection algorithms. The proposed matrix inversion technique is integrated into linear as well as selection-based list detection algorithms for lower latency and deeper parallelism. Then our analysis of the impact of channel hardening on selection-based list detection motivates the use of an improved ordering scheme for the successive interference cancellation sub-detector. Finally, we compare our improved selection-based list detector with other two state-of-art low complexity LS-MIMO detection algorithms, namely, multistage likelihood ascent search (LAS) and message passing detection (MPD). Computer simulations show that the proposed selection-based list detector performs better than multistage LAS and has just a small fraction of dB performance loss compared with MPD. Because of its good performance and parallelizable nature, the proposed algorithm offers an attractive alternative for detection in practical LS-MIMO systems.

INDEX TERMS Large-scale MIMO, MIMO detection, channel hardening, multiple antenna systems.

I. INTRODUCTION

The sharp increase of multimedia data traffic in wireless communications and the shortage of radio spectrum motivate the need for novel technologies that can accommodate this trend while providing high performance. Constituting a principal technology for fifth generation (5G) wireless communication systems, large-scale multiple-input multiple-output (LS-MIMO) is a candidate for providing advantages in spectral and energy efficiency, link reliability and system robustness [1]–[3]. A principal application of LS-MIMO is envisaged to be in multi-user (MU) base stations (BS) for 5G wireless communications. The usual application of LS-MIMO in wireless communication systems involves a large number of transmit (N_t) and receive (N_r) antennas, creating a channel that can be represented by a large $N_r \times N_t$ matrix. However, such a model can arise also when a small number of antennas is used. For example [4] introduces a unified matrix representation (UMR) for MIMO systems with high order QAM, that transforms the original scheme into a MIMO system with binary inputs at the expense of increasing the size of the transmitted vector. The transformed MIMO matrix could correspond to an LS-MIMO system. Even some single antenna systems can be represented as LS-MIMO. In [5] an OFDM system employing K subcarriers is represented in the frequency domain as $K \times K$ MIMO allowing the derivation of a detection technique based on sphere decoding. Since K, the number of subcarriers in OFDM, is usually very large we essentially have an LS-MIMO system.

Although LS-MIMO technology can provide significant benefits, issues still exist for its use in practical communication systems. One that is of paramount importance is the design of high performance detectors for the uplink. Techniques such as maximum likelihood detection (MLD) [6] and the sphere decoder (SD) [7] have asymptotic complexities that become prohibitively high when the number of transmit antennas increases [6], [8], and hence are infeasible for practical LS-MIMO. Furthermore, the basic SD algorithm is not amenable for parallel implementation [9].

However, [9] presents some intersting modifications to SD, employing lattice reduction techniques, that bridge the power efficiency performance between SD and detection structures based on minimum mean squared error (MMSE) successive interference cancellation (SIC), while allowing for a parallel implementation. The complexity analysis in [9] has been done through computer simulations for conventional size MIMO schemes only. An improvement over MMSE-SIC detection is presented in [10] where a ''shadow area'' is employed to determine symbol reliability. When a soft symbol estimate belongs to the shadow area it is categorized as unreliable and a candidate list is used to decide which symbol was transmitted. Another list based detection method is presented in [11] where multiple feedforward and decision feedback sections are used to form a list of improved detection candidates. In recent years, several lower complexity high performance detectors were proposed for LS-MIMO systems, such as the block-iterative generalized decision feedback equalizer (BI-GDFE) [12]–[14], likelihood ascend search (LAS) [15]–[17], reactive tabu search (RTS) [18], [19], message passing detectors (MPD) [20]–[22], low complexity approximate MPD [23], Monte-Carlo sampling algorithms [24], and element-based lattice reduction (ELR) aided linear detectors [25].

Selection based list detection for LS-MIMO has the advantage of massively parallelization [26]–[28], allowing for high data throughput implementations. In general, selection based list detection consists of three stages: channel partition, candidate list generation and final decision. At the channel partition stage, the channel is partitioned into two subsets based on a certain selection scheme. At the candidate list generation stage, for the first channel subset, all the hypotheses of the corresponding transmitted data sub-vectors are considered, while for the second channel subset, the decisions of the symbol sub-vector are obtained by a low complexity scheme such as a linear detector (LD) or its SIC counterparts. Then the best candidate in the list, using the minimum Euclidean distance (MED) rule, is chosen as the final decision. In [26], a selection based list algorithm called generalized parallel interference cancellation (GPIC) was proposed, which performs channel partition by considering the postprocessing signal to noise ratio (SNR) using the zero forcing (ZF) criterion. In [27] it is shown theoretically that the channel partition procedure is crucial for good performance of selection based list detection in conventional small MIMO. Radji and Leib [27] proposed an improved scheme of GPIC, named Sel-MMSE-OSIC, that exploits diversity maximization channel selection (DMS) for channel partition and derived a sufficient condition to achieve optimal asymptotic diversity. The scheme of [28] uses a simpler incremental channel partition technique for replacing DMS and employs a tree search algorithm for candidate list generation, reducing complexity compared with Sel-MMSE-OSIC. More recently [29] presented a list based MIMO detection technique in the spirit of [26]–[28] also using the concept of patitioning the input signal vector in order to reduce complexity. Unlike [26]–[28], however, in [29] the patitioning could be in more than two groups. These schemes can provide a performance close to MLD in conventional small and medium size MIMO systems.

In this work we consider the adaptation of the schemes from [27] and [28] to LS-MIMO applications, by using approximate matrix inversion and exploiting the channel hardening phenomenon at various detection stages. The schemes in [27] and [28] are designed to provide optimal diversity that is very large in LS-MIMO systems [6], and realized at very high SNR. However, such asymptotic diversity may never be achieved over practical SNR ranges in LS-MIMO systems. A significant factor that contributes to complexity in selection based list detection is the size of the candidate list. In LS-MIMO systems it is important to have good diversity over practical BER ranges (i.e. no less than 10^{-7}) while ensuring the size of the candidate list is feasible for implementation.

Complex matrix inversion is widely used not only in selection based list detection, but also in other detection techniques for LS-MIMO systems. However, even for conventional MIMO systems complex matrix inversion is cumbersome to implement [30], [31]. It is worth pointing out that in practical implementation of detection algorithms, the measure of asymptotic complexity is not sufficient. Processing latency (parallel time units), memory consumption, power consumption and hardware cost are also important measures. Generally speaking, exact matrix inversion schemes, such as Gaussian Elimination (GE), Cholesky decomposition (CD) and QR decomposition based algorithms, require $\mathbb{O}(N_t)$ parallel time units [30] that might exceed the channel coherence interval. In order to address this issue, the channel hardening phenomenon [1], [32] can be used to approximate matrix inversion based on L-term Neumann series expansion (SE) for LS-MIMO detection [33], [34]. An interesting aspect of channel hardening is that when the system loading factor $\alpha = \frac{N_t}{N_r}$ decreases, the orthogonality between the columns of the channel matrix increases, making the diagonal components of the associated Gram matrix stronger compared with the off diagonal components (i.e. the Gram matrix becomes closer to diagonal). Based on this quasi-diagonal structure of the Gram matrix, the L-term SE approximation enables parallel and efficient hardware implementations [33], [34]. Nevertheless, there are two major drawbacks of L-term SE approximation that hinder its practical usage. Firstly, the conventional L-term SE approximation converges to the exact matrix inverse slowly (linearly). Secondly, the L-term SE approximation is only valid when the system loading factor satisfies a convergence condition [35], possing a limit to spatial multiplexing gains.

In this paper, we first introduce a refined approximate matrix inversion technique based on 2-term SE approximation and Newton Iteration [36]–[39], named K-step series expansion Newton iteration approximation (K-SENIA). The proposed technique converges faster (exponentially) than the conventional L-term SE approximation. We further relax the convergence constraint of K-SENIA by using matrix

inversion inflate updates (IU) [40], allowing for higher system loading factors to be achieved. The K-SENIA technique is integrated into linear as well as selection based list algorithms, enabling deeper parallelization. Then we analyse the impact of channel hardening on selection based list algorithms. We show that when the dimension of the channel matrix increases, the DMS rule and V-BLAST ordering for SIC based on the postprocessing SINR of data substreams become less effective. Furthermore, we find that in medium size LS-MIMO systems (e.g. 128×32 and 128×96), ordering has a larger impact on performance than channel partition. Capitalizing on these results, we propose an improved selection based list algorithm by employing Type-L reliability ordering [41] in SIC sub-detectors. Simulation results reveal significant performance improvement of this approach.

The rest of the paper is organized as follows. Section II introduces the system model as well as the K-SENIA/IU scheme and their complexity/latency analysis. The impact of channel hardening on selection based list detection in LS-MIMO is analyzed in section III. Section IV presents the improved selection based list detection technique. A comparison of the improved selection based list detection, multi-stage LAS algorithm [15], [42], MPD [22], as well as other schemes, is provided in section V. Section VI concludes this paper.

II. LARGE-SCALE MIMO SYSTEMS AND APPROXIMATE MATRIX INVERSION

A. SYSTEM MODEL AND THE CHANNELL HARDENING PHENOMENON

Consider an uncoded complex LS-MIMO MU uplink system with N_r BS antennas serving N_t single antenna users, and system loading factor $\alpha = \frac{N_t}{N_r}$. Independent information streams from each user, in form of bit sequences, are mapped to complex symbols in groups of n_c consecutive bits. The complex symbols are statistically independent belonging to a finite signal constellation alphabet $\mathbb{A}$ (e.g., BPSK, 4-QAM, 16-QAM, 64-QAM) of size $|\mathbb{A}| = M = 2^{n_c}$ with average energy E_s. Then the complex symbols are transmitted by N_t antennas over a Rayleigh flat fading matrix channel. With perfect synchronization between receiving and transmission sides, the generic discrete time model for the MIMO system is given by:

$$\mathbf{y} = \mathbf{H}\mathbf{s} + \mathbf{n}, \tag{1}$$

where $\mathbf{y} \in \mathbb{C}^{N_r\times1}$ is the received signal vector, and $\mathbf{s} \in \mathbb{C}^{N_t\times1}$ is the transmitted symbol vector. Each component of $\mathbf{s}$ is independently drawn from $\mathbb{A}$ with equal probability, satisfying $\mathbb{E}[\mathbf{s}\mathbf{s}^H] = \mathbf{I}_{N_t}E_s$, where $\mathbb{E}[\cdot]$ denotes the expectation operation, $(\cdot)^H$ denotes the Hermitian transpose, and $\mathbf{I}_{N_t}$ is the identity matrix of size $N_t \times N_t$. Furthermore $\mathbf{H} \in \mathbb{C}^{N_r\times N_t}$ is the Rayleigh fading channel matrix, and $[\mathbf{H}]_{ij}$ is the component of $\mathbf{H}$ on the ith row and jth column, representing the fading coefficient from the jth transmit to the ith receive antenna. The components of $\mathbf{H}$ are independent identically distributed (i.i.d) circularly symmetric complex Gaussian (CSCG) with zero mean and unit variance, $[\mathbf{H}]_{ij} \sim \mathbb{C}\mathcal{N}(0,1)$. Finally, $\mathbf{n} \in \mathbb{C}^{N_r\times1}$ is an additive white Gaussian noise (AWGN) vector with i.i.d CSCG independent components of zero mean and variance σ_o^2, satisfying $\mathbb{E}[\mathbf{n}\mathbf{n}^H] = \mathbf{I}_{N_r}\sigma_o^2$. The average symbol signal to noise ratio (SNR) is $\rho_s = \frac{E_s}{\sigma_o^2}$, and the average SNR at each receive antenna is $\rho_r = \frac{N_tE_s}{\sigma_o^2}$. The task of a MIMO detector is to estimate $\mathbf{s}$, based on the received vector $\mathbf{y}$ and channel propagation matrix $\mathbf{H}$.

Linear detectors (LD), known for their low complexity [6], generate soft estimates of the transmitted vector $\mathbf{s}$ by applying a linear transformation on $\mathbf{y}$ and then quantizing each component of the soft estimate to the closest point in the symbol constellation $\mathbb{A}$. Let $\mathbf{G} \in \mathbb{C}^{N_t\times N_r}$ be the linear transformation matrix, and $\hat{\mathbf{s}}^{LD}$ denote the output of the LD, then the LD is given by

$$\hat{\mathbf{s}}^{LD} = \mathcal{Q}[\mathbf{G}\mathbf{y}], \tag{2}$$

where $\mathcal{Q}[\cdot]$ denotes the quantization operator. Popular LDs are zero forcing (ZF) and minimum mean square error (MMSE) detectors [6] with matrices $\mathbf{G}_{ZF} = (\mathbf{H}^H\mathbf{H})^{-1}\mathbf{H}^H$ and $\mathbf{G}_{MMSE} = (\mathbf{H}^H\mathbf{H} + \rho_s^{-1}\mathbf{I})^{-1}\mathbf{H}^H$ respectively. Successive interference cancellation (SIC), also known as nulling-cancelling, may improve the error performance of an LD. With SIC, the interference in the soft estimate produced by the LD is cancelled from the received signal vector, thus increasing the reliabilities of the remaining estimates. Since MMSE-SIC techniques can achieve significant performance gains over ZF-SIC [43], [44], in this work we consider MMSE-SIC.

Next consider the channel hardening phenomenon. Based on the Marčenko-Pastur law [45], when $N_r, N_t \to \infty$, with α fixed, the empirical distribution of the eigenvalues of the Gram matrix $\mathbf{W} = \mathbf{H}^H\mathbf{H}$ converges to a fixed distribution. Following [46], let $\lambda_{max}(\mathbf{X})$ and $\lambda_{min}(\mathbf{X})$ denote the largest and smallest eigenvalues of $\mathbf{X}$ respectively. When N_r, $N_t \to \infty$, we have

$$\lambda_{max}(\mathbf{W}) \to N_r(1+\sqrt{\alpha})^2, \quad \lambda_{min}(\mathbf{W}) \to N_r(1-\sqrt{\alpha})^2, \tag{3}$$

that yields

$$\begin{aligned}\lambda_{max}\left(\frac{1}{N_r(1+\alpha)}\mathbf{W}\right) &\to \left(1+\frac{2\sqrt{\alpha}}{1+\alpha}\right),\\ \lambda_{min}\left(\frac{1}{N_r(1+\alpha)}\mathbf{W}\right) &\to \left(1-\frac{2\sqrt{\alpha}}{1+\alpha}\right).\end{aligned} \tag{4}$$

From (4), we see that the eigenvalues of $\mathbf{I}_{N_t} - \frac{1}{N_r(1+\alpha)}\mathbf{W} = \mathbf{I}_{N_t} - \frac{1}{N_r+N_t}\mathbf{W}$, lie approximately in the range of $[\frac{-2\sqrt{\alpha}}{1+\alpha}, \frac{2\sqrt{\alpha}}{1+\alpha}]$. If $\alpha \to 0$, then $[\frac{-2\sqrt{\alpha}}{1+\alpha}, \frac{2\sqrt{\alpha}}{1+\alpha}] \to [0,0]$, and using the eigendecomposition [47] of $\mathbf{I}_{N_t} - \frac{1}{N_r+N_t}\mathbf{W}$, we have

$$\lim_{N_r,N_t\to\infty,\alpha\to0}\left(\mathbf{I}_{N_t} - \frac{1}{N_r+N_t}\mathbf{W}\right) = \mathbf{0}, \tag{5}$$

where $\mathbf{0}$ is the zero matrix. Then from (5)

$$\lim_{N_r,N_t\to\infty,\alpha\to0}\mathbf{W} = (N_r+N_t)\mathbf{I}_{N_t} \overset{N_r\gg N_t}{=} N_r\mathbf{I}_{N_t}, \tag{6}$$

indicating that when N_r and N_t both grow to infinity and $\alpha = \frac{N_t}{N_r} \to 0$, $\mathbf{W}$ converges to a diagonal matrix. The diagonal dominance structure of $\mathbf{W}$ allows exploitation of the Neumann series expansion to approximate $\mathbf{W}^{-1}$ in various MIMO detection schemes.

B. IMPROVED APPROXIMATE MATRIX INVERSION EXPLOITING CHANNELL HARDENING

Next, we present an improved approximate matrix inversion scheme, K-SENIA, based on conventional 2-term SE and Newton iteration, that converges to the exact matrix invers with exponential speed, and uses an inflate update (IU) technique to handle the cases where convergence conditions are not satisfied.

1) NEUMANN SERIES EXPANSION AND nEWTON ITERATION

Consider invertible matrices $\mathbf{A} \in \mathbb{C}^{N\times N}$ and $\mathbf{X} \in \mathbb{C}^{N\times N}$, that satisfy $\lim_{L\to\infty}(\mathbf{I} - \mathbf{X}^{-1}\mathbf{A})^L = \mathbf{0}$. Then we have [33]

$$(\mathbf{X}^{-1}\mathbf{A})^{-1} = \sum_{n=0}^{\infty}(\mathbf{I} - \mathbf{X}^{-1}\mathbf{A})^n, \tag{7}$$

and hence

$$\mathbf{A}^{-1} = \sum_{n=0}^{\infty}(\mathbf{I} - \mathbf{X}^{-1}\mathbf{A})^n\mathbf{X}^{-1}. \tag{8}$$

The L-term SE approximation of $\mathbf{A}^{-1}$, denoted by $\tilde{\mathbf{A}}_L^{-1}$, is given by

$$\tilde{\mathbf{A}}_L^{-1} = \sum_{n=0}^{L-1}(\mathbf{I} - \mathbf{X}^{-1}\mathbf{A})^n\mathbf{X}^{-1}, \tag{9}$$

and the approximation residual matrix of $\tilde{\mathbf{A}}_L^{-1}$, is

$$\tilde{\mathbf{R}}_L = \mathbf{I} - \tilde{\mathbf{A}}_L^{-1}\mathbf{A} = (\mathbf{I} - \mathbf{X}^{-1}\mathbf{A})^L. \tag{10}$$

The Gram matrix can be decomposed as $\mathbf{W} = \mathbf{D} + \mathbf{E}$, where $\mathbf{D}$ is diagonal with diagonal components that are those of $\mathbf{W}$, and $\mathbf{E}$ is a zero diagonal matrix with the off diagonal components of $\mathbf{W}$. With $\mathbf{A} = \mathbf{W}$ and $\mathbf{X} = \mathbf{D}$, in (9), the L-term SE approximation of $\mathbf{W}^{-1}$ is

$$\tilde{\mathbf{W}}_L^{-1} = \sum_{n=0}^{L-1}(-\mathbf{D}^{-1}\mathbf{E})^n\mathbf{D}^{-1}. \tag{11}$$

Based on (10), the L-term approximation residual matrix of $\tilde{\mathbf{W}}_L^{-1}$, denoted by $\tilde{\mathbf{R}}_L$, is given by

$$\tilde{\mathbf{R}}_L = (-\mathbf{D}^{-1}\mathbf{E})^L. \tag{12}$$

If $N_r, N_t \to \infty, \alpha \to 0$, $\mathbf{W}$ becomes diagonal as shown in (6) and $\mathbf{D}^{-1}\mathbf{E}$ tends to $\mathbf{0}$. Then $\tilde{\mathbf{R}}_L$ in (12) becomes $\mathbf{0}$, so we can conclude that the performance of L-term SE approximation improves when the system loading factor α decreases or L increases [35]. Furthermore, the condition for α ensuring asymptotic convergence of the SE approximation (i.e., $\lim_{L\to\infty}\tilde{\mathbf{W}}_L^{-1} = \mathbf{W}^{-1}$) with high probability is $\alpha < (\sqrt{2}-1)^2$ [35]. Consider the 2-term SE approximation $\tilde{\mathbf{W}}_2^{-1} = \mathbf{D}^{-1} - \mathbf{D}^{-1}\mathbf{E}\mathbf{D}^{-1}$ and notice that $\mathbf{D}^{-1}$ is a diagonal matrix. Thus the computation of $\tilde{\mathbf{W}}_2^{-1}$ only requires scalar-vector multiplications, with complexity in order of $\mathbb{O}(N_t^2)$.

Newton iteration is a recursive matrix inverse approximation method [36]–[38], that converges fast, is massively parallelizable, and has good numerical stability. Let $\mathbf{M}_{k+1}$ denote the approximate matrix inverse computed by Newton iteration at step $k+1$. Then

$$\mathbf{M}_{k+1} = (2\mathbf{I} - \mathbf{M}_k\mathbf{A})\mathbf{M}_k, \quad k = 0, 1, 2, \ldots \tag{13}$$

and the approximation residual matrix at step $k+1$ is

$$\mathbf{R}_{k+1} = \mathbf{I} - \mathbf{M}_{k+1}\mathbf{A} = (\mathbf{I} - \mathbf{M}_k\mathbf{A})^2 = \mathbf{R}_k^2. \tag{14}$$

Therefore, the Newton iteration scheme converges with exponential speed.

The conventional L-term SE approximation can be refined by using the Newton iteration method. The more computationally simple approximation $\tilde{\mathbf{W}}_2^{-1}$ is used as the initial input to Newton iteration, that is denoted by $\check{\mathbf{M}}_0$. Let $\check{\mathbf{M}}_k$ denote the refined output after the kth step Newton iteration. With $\check{\mathbf{M}}_k = \tilde{\mathbf{W}}_L^{-1}$ from (11) and using (10) and (13) we have

$$\begin{aligned}\check{\mathbf{M}}_{k+1} &= (2\mathbf{I} - \check{\mathbf{M}}_k\mathbf{W})\check{\mathbf{M}}_k = (\mathbf{I} + \mathbf{I} - \tilde{\mathbf{W}}_L^{-1}\mathbf{W})\tilde{\mathbf{W}}_L^{-1} \\ &= (\mathbf{I} + \tilde{\mathbf{R}}_L)\tilde{\mathbf{W}}_L^{-1}.\end{aligned} \tag{15}$$

Then the use of (11) and (12) in (15) yields

$$\check{\mathbf{M}}_{k+1} = \sum_{n=0}^{L-1}(-\mathbf{D}^{-1}\mathbf{E})^n\mathbf{D}^{-1} + \sum_{n=L}^{2L-1}(-\mathbf{D}^{-1}\mathbf{E})^n\mathbf{D}^{-1} = \tilde{\mathbf{W}}_{2L}^{-1}. \tag{16}$$

From (15) and (16) we have $\tilde{\mathbf{W}}_{2L}^{-1} = (\mathbf{I} + \tilde{\mathbf{R}}_L)\tilde{\mathbf{W}}_L^{-1}$. With $L = 2^k$ we have

$$\tilde{\mathbf{W}}_{2^{k+1}} = (\mathbf{I} + \tilde{\mathbf{R}}_{2^k})\tilde{\mathbf{W}}_{2^k}^{-1} \tag{17}$$

and from (12)

$$\tilde{\mathbf{R}}_{2^k} = (-\mathbf{D}^{-1}\mathbf{E})^{2^k}. \tag{18}$$

Hence starting with $\tilde{\mathbf{W}}_2^{-1}$ and using the iterations (17) (18) we can calculate an approximation to $\tilde{\mathbf{W}}^{-1}$. Hereinafter this technique is termed as the K-term series expansion Newton iterative approximation (K-SENIA), where K denotes the number of Newton iterations.

2) ACHIEVING HIGHER SYSTEM LOADING FACTOR MATRIX INVERSION INFLATE UPDATE (IU)

Similarly to conventional L-term SE approximation, K-SENIA is only effective for LS-MIMO with α satisfying the asymptotic convergence condition (if $\alpha < (\sqrt{2}-1)^2$ then $\lim_{L\to\infty}\tilde{\mathbf{W}}_L^{-1} = \mathbf{W}^{-1}$ with high probability [35]). This convergence condition is very strict and significantly limits the spatial multiplexing gain. Next we propose a scheme that combines a matrix inversion inflate update (IU) technique with K-SENIA that relaxes this convergence constraint.

When the channel matrix is modified by adding a new column, IU efficiently updates the inflated Gram matrix

inverse from the previous inverse, rather than recomputing it from scratch [40]. We extend the ZF-IU technique from [40] to MMSE-IU. Assume $\mathbf{W}^{-1} = (\mathbf{H}^H\mathbf{H}+\rho^{-1}\mathbf{I}_{N_t})^{-1}$ is already computed. Then a new column $\mathbf{h}_n$ is added to $\mathbf{H}$, resulting in the new inflated matrix $\mathbf{H}_e = [\mathbf{H}, \mathbf{h}_n]$. To find $\mathbf{W}_e^{-1} = (\mathbf{H}_e^H\mathbf{H}_e + \rho^{-1}\mathbf{I}_{N_t+1})^{-1}$, notice that

$$\mathbf{W}_e^{-1} = \begin{bmatrix} \mathbf{H}^H\mathbf{H} + \rho^{-1}\mathbf{I}_{N_t}, & \mathbf{H}^H\mathbf{h}_n \\ \mathbf{h}_n^H\mathbf{H}, & \mathbf{h}_n^H\mathbf{h}_n + \rho^{-1} \end{bmatrix}^{-1}. \quad (19)$$

Using the inverse of the partitioned matrix and Sherman-Morrison formula [48], we have

$$\mathbf{W}_e^{-1} = \begin{bmatrix} \mathbf{F}_{11}^{-1}, & -c\mathbf{W}^{-1}\mathbf{H}^H\mathbf{h}_n \\ -c\mathbf{h}_n^H\mathbf{H}\mathbf{W}^{-1}, & c \end{bmatrix}, \quad (20)$$

where

$$c = 1/(\mathbf{h}_n^H\mathbf{h}_n + \rho^{-1} - \mathbf{h}_n^H\mathbf{H}\mathbf{W}^{-1}\mathbf{H}^H\mathbf{h}_n), \quad (21)$$
$$\mathbf{F}_{11}^{-1} = \mathbf{W}^{-1} + c\mathbf{W}^{-1}\mathbf{H}^H\mathbf{h}_n\mathbf{h}_n^H\mathbf{H}\mathbf{W}^{-1}. \quad (22)$$

Therefore, each IU step calculating $\tilde{\mathbf{W}}_e^{-1}$ can be summarized as:

$$\begin{aligned} \mathbf{t}_1 &= \mathbf{H}^H\mathbf{h}_n, \\ \mathbf{t}_2 &= \mathbf{W}^{-1}\mathbf{t}_1, \\ c &= 1/(\mathbf{h}_n^H\mathbf{h}_n + \rho^{-1} - \mathbf{t}_1^H\mathbf{t}_2), \mathbf{t}_3 = -c\mathbf{t}_2, \\ \mathbf{F}_{11}^{-1} &= \mathbf{W}^{-1} + c\mathbf{t}_2\mathbf{t}_2^H, \quad \mathbf{W}_e^{-1} = \begin{bmatrix} \mathbf{F}_{11}^{-1}, & \mathbf{t}_3 \\ \mathbf{t}_3^H, & c \end{bmatrix}, \end{aligned}$$

where only vector wise multiplication is required. The combined scheme of K-SENIA and IU is termed as K-SENIA-IU. Capitalizing on the fact that a good approximation can be achieved by K-SENIA in MIMO systems with α satisfying the convergence condition [35], the K-SENIA inverse for a sub-matrix composed of arbitrary N_i columns from $\mathbf{H}$, is firstly computed and fed to IU as the initial input. Then the matrix inverse is updated using IU by adding the remaining channel columns. To elaborate further, assume a LS-MIMO MU system whose loading factor exceeds the asymptotic convergence constraint. First the channel matrix $\mathbf{H}$ is partitioned into two sub channel matrices $\mathbf{H}_{ini}$ and $\mathbf{H}_{rem}$. The matrix $\mathbf{H}_{ini} \in \mathbb{C}^{N_r\times N_i}$ consists of arbitrary N_i columns of $\mathbf{H}$, where $\frac{N_i}{N_r}$ satisfies the convergence condition [35], and $\mathbf{H}_{rem} \in \mathbb{C}^{N_r\times(N_t-N_i)}$ is composed of the remaining columns from $\mathbf{H}$. Then K-SENIA is used to approximate $(\mathbf{H}_{ini}^H\mathbf{H}_{ini} + \rho^{-1}\mathbf{I}_{N_i})^{-1}$, resulting in $\check{\mathbf{W}}_{N_i}^{-1}$. Finally IU is used recursively to update $\check{\mathbf{W}}_{N_i}^{-1}$ by adding the remaining columns from $\mathbf{H}_{rem}$, until $\check{\mathbf{W}}_{N_t}^{-1}$ is obtained. Let $\check{\mathbf{W}}_{N_i+j}^{-1}$ denote the updated matrix inverse at the jth step with $j = 1, 2, \ldots, N_t - N_i$. The K-SENIA-IU procedure is specified by Algorithm 1.

Algorithm 1 Pseudo Code of K-SENIA-IU

procedure K-SENIA-IU($\mathbf{H}$, ρ_r, N_i)
  Partition $\mathbf{H}$ into $\mathbf{H}_{ini} \in \mathbb{C}^{N_r\times N_i}$ and $\mathbf{H}_{rem} \in \mathbb{C}^{N_r\times(N_t-N_i)}$
  $\mathbf{W}_{N_i} \leftarrow \mathbf{H}_{ini}^H\mathbf{H}_{ini} + \rho_r^{-1}\mathbf{I}_{N_i}$
  $\check{\mathbf{W}}_{N_i}^{-1} \leftarrow K\text{-}SENIA(\mathbf{W}_{N_i}, k)$ ▷ Compute $\check{\mathbf{W}}_{N_i}^{-1}$ via K-SENIA
  $\mathbf{H}_{curr} \leftarrow \mathbf{H}_{ini}$
  for $j \leftarrow 1$ to $(N_t - N_i)$ **do**
    $\check{\mathbf{W}}_{N_i+j}^{-1} \leftarrow \mathbf{IU}(\check{\mathbf{W}}_{N_i+j-1}^{-1})$ ▷ update the matrix inverse via IU
    $\mathbf{H}_{curr} \leftarrow [\mathbf{H}_{curr}, \mathbf{h}_{p^i}]$ ▷ Inflate $\mathbf{H}_{curr}$ by adding column $\mathbf{h}_{p^i}$, which is extracted from $\mathbf{H}_{rem}$
  end for
  return $\check{\mathbf{W}}_{N_t}^{-1}$
end procedure

3) COMPLEXITY AND LATENCY ANALYSIS OF K-SENIA, AND IU

Similarly to [15], complexity in this work is defined as the number of complex arithmetic operations. The K-SENIA scheme consists of two main parts. The first part is the computation of $\tilde{\mathbf{W}}_2^{-1}$, which only requires scalar-vector multiplication, with complexity that scales as $\mathbb{O}(N_t^2)$. The second part consists of k step Newton iterations, that each requires two matrix-matrix multiplications with complexity that scales as $\mathbb{O}(2N_t^3)$. Therefore the overall complexity of K-SENIA is of order $\mathbb{O}(2kN_t^3)$, the same as exact matrix inversion. Concerning processing latency, matrix-matrix multiplication requires $\mathbb{O}(\log(N_t))$ parallel time units [37] and the latency of computing $\tilde{\mathbf{W}}_2^{-1}$ is negligible compared with matrix-matrix multiplication [33]. Thus the processing latency of K-SENIA scales as $\mathbb{O}(2k\log(N_t))$. With a 2^{k+1}-term SE approximation, a 2^{k+1}-term expansion is required. The 2^{k+1}-term SE approximation consists of two main parts. The first part is the computation of $\tilde{\mathbf{W}}_2^{-1}$, with complexity $\mathbb{O}(N_t^2)$ and negligible processing latency compared with matrix-matrix multiplication. Secondly, $\tilde{\mathbf{W}}_{2^{k+1}}^{-1}$ of (11) is updated by $\tilde{\mathbf{W}}_{2^{k+1}}^{-1} = (-\mathbf{D}^{-1}\mathbf{E})\tilde{\mathbf{W}}_{2^{k+1}-1}^{-1} + \mathbf{D}^{-1}$, thus in total $2^{k+1}-2$ matrix-matrix multiplications are required. We conclude that K-SENIA requires $2k$ matrix-matrix multiplications, while 2^{k+1}-term SE approximation requires $2^{k+1}-2$ matrix-matrix multiplications. The complexity and latency gain of K-SENIA over 2^{k+1}-term SE approximation are both $\frac{2^k-1}{k}$.

Consider IU of Algorithm 1, with the initial approximate matrix invers $\check{\mathbf{W}}_{N_i}^{-1} \in \mathbb{C}^{N_i\times N_i}$. To obtain $\check{\mathbf{W}}_{N_t}^{-1}$ there are $N_t - N_i$ IU steps, and at the jth step, with $\check{\mathbf{W}}_{N_i+j-1}^{-1} \in \mathbb{C}^{(N_i+j-1)\times(N_i+j-1)}$ to be updated, the computation complexities of $\mathbf{t}_1, \mathbf{t}_2$ and $\mathbf{t}_3$ scale as $\mathbb{O}(N_r(N_i+j-1))$, $\mathbb{O}((N_i+j-1)^2)$ and $\mathbb{O}(N_i+j-1)$ respectively. Then the complexity of computing c is of order $\mathbb{O}(N_r+N_i+j-1)$. Finally, the complexity of computing $\mathbf{F}_{11}^{-1}$ is of order $\mathbb{O}((N_i+j-1)^2)$. Therefore, the overall complexity required by the jth IU step is of order $\mathbb{O}(N_r(N_i+j-1))$. Concerning processing latency, notice that IU only requires matrix-vector and vector-vector multiplication, thus compared with K-SENIA the latency of IU can be ignored. Then we consider the complexity of K-SENIA-IU. The computation of $\check{\mathbf{W}}_{N_i}^{-1}$ by K-SENIA

requires a complexity of order $\mathbb{O}(2kN_i^3)$, and the complexity of $N_t - N_i$ steps of IU is of order $\mathbb{O}(N_rN_t^2 - N_rN_i^2)$ (the complexity of the jth step is of order $\mathbb{O}(N_r(N_i+j-1))$, for $j = 1, 2, \cdots, N_t - N_i$, the overall complexity is of order $\sum_{j=1}^{N_t-N_i}\mathbb{O}(N_r(N_i+j-1)) = \mathbb{O}(N_rN_t^2 - N_rN_i^2)$). Thus the overall complexity of K-SENIA-IU scales as $\mathbb{O}(N_rN_t^2)$ $(\mathbb{O}(N_rN_t^2 - N_rN_i^2) + \mathbb{O}(2kN_i^3) = \mathbb{O}(N_rN_t^2 + (2kN_i - N_r)N_i^2)$. Since $2kN_i$ is close to N_r, the overall complexity after simplification is of order $\mathbb{O}(N_rN_t^2))$, the same as that of exact matrix inversion.

From the analysis above, we can see that the processing latency of K-SENIA scales as $\mathbb{O}(2k\log(N_t))$, that is much lower than that of exact matrix inversion schemes $(\mathbb{O}(N_t))$ when N_t is large. In [33], it is shown that the VLSI implementation of the matrix multiplication based SE approximate matrix inversion can save hardware resources compared with Cholesky decomposition based exact matrix inversions. In addition, K-SENIA and IU only require scalar-vector, matrix-vector and matrix-matrix multiplications, that can be implemented using generic, parallelizable and reusable Multiply-and-Accumulated (MAC) structures, while QR decomposition based exact matrix inversions require complicated data flow mechanism and arithmetic operation units (e.g., square root, sin/cos functions) [30]. Finally, [34] shows that hardware implementation of SE approximate matrix inversion is more energy efficient than that of QR decomposition based exact matrix inversions.

C. APPLICATIONS OF IMPROVED APPROXIMATE MATRIX INVERSION TO LINEAR MMSE DETECTION

In order to assess the performance of the approximate matrix inversion technique for detection in LS-MIMO, in this section we consider a simple MMSE detector which is capable of achieving near-optimal performance in low loaded (very small α) systems with low complexity $\mathbf{O}(N_rN_t^2)$ [15], and hence considered for practical applications [2]. We start by characterizing the approximation error in the estimated transmitted symbol vector when exact matrix inversion is replaced by K-SENIA resulting in MMSE-SENIA. For LDs with approximate matrix inversions, at low SNR the multiuser interference (MUI) and noise are the dominant factors influencing performance [39], and obscuring the errors of approximate matrix inversion. Thus our analysis is carried out at high SNR ($\rho_r \to \infty$), where the approximation errors become dominant. Assume the convergence condition is satisfied (i.e, $\mathbf{W}^{-1} = \tilde{\mathbf{W}}_{\infty}^{-1}$) and let $\mathbf{W}_{\triangle}^{-1}$ denote the approximation error matrix of K-SENIA

$$\mathbf{W}_{\triangle}^{-1} = \mathbf{W}^{-1} - \tilde{\mathbf{W}}_{2^{k+1}}^{-1}, \tag{23}$$

where $\mathbf{W}^{-1} = \tilde{\mathbf{W}}_{\infty}^{-1}$. The use of (11) in (23) yields

$$\begin{aligned}\mathbf{W}_{\triangle}^{-1} &= \sum_{n=2^{k+1}}^{\infty}(-\mathbf{D}^{-1}\mathbf{E})^n\mathbf{D}^{-1} \\ &= (-\mathbf{D}^{-1}\mathbf{E})^{2^{k+1}}\sum_{n=0}^{\infty}(-\mathbf{D}^{-1}\mathbf{E})^n\mathbf{D}^{-1} \\ &= (-\mathbf{D}^{-1}\mathbf{E})^{2^{k+1}}\mathbf{W}^{-1}.\end{aligned} \tag{24}$$

Let $\mathbf{W} = \mathbf{H}^H\mathbf{H} + \rho_s^{-1}\mathbf{I}$ denote the regularized Gram matrix. The soft estimates of the original MMSE detector and MMSE detector with K-SENIA, denoted by $\hat{\mathbf{s}}^{MMSE}$ and $\hat{\mathbf{s}}^{MMSE-SENIA}$ respectively, are given by $\hat{\mathbf{s}}^{MMSE} = \mathbf{W}^{-1}\mathbf{H}^H\mathbf{y}$ and $\hat{\mathbf{s}}^{MMSE-SENIA} = \tilde{\mathbf{W}}_{2^{k+1}}^{-1}\mathbf{H}^H\mathbf{y}$. The mean square error (MSE) ϵ of this approximation is defined as

$$\epsilon = \mathbb{E}(||\hat{\mathbf{s}}^{MMSE} - \hat{\mathbf{s}}^{MMSE-SENIA}||^2), \tag{25}$$

and at high SNR

$$\epsilon_{\infty} = E_s\mathbb{E}[||(\mathbf{D}^{-1}\mathbf{E})^{2^{k+1}}||_F^2]. \tag{26}$$

where $||\cdot||_F$ denotes the Frobenius norm.

Proof: see Appendix A.

The insights provided by (26) are twofold. Firstly, since $\epsilon_{\infty} > 0$, the existence of an error floor in the BER-SNR curves of MMSE-SENIA at high SNR is expected. Secondly, the level of the error floor is determined by two factors: the number of iteration of K-SENIA, and how close the components in $(\mathbf{D}^{-1}\mathbf{E})^{2^{k+1}}$ are to zero.

In Fig. 1, we present the BER performance of MMSE-SENIAk, where k denotes the number of iterations, in 128×16 and 32×4 16-QAM MIMO systems, where the convergence condition are satisfied. For comparison, the performances of a MMSE detector with exact matrix inversion, referred to as MMSE-EMI and that of a MMSE detector using a 3-term SE approximation, referred to as MMSE-SE3 are also presented. We see from Fig. 1 that MMSE-SENIA with $k = 1, 2, 3$ outperforms MMSE-SE3 significantly. In the 128×16 MIMO system, at BER $= 6.8 \times 10^{-4}$, the SNR gains provided by MMSE-SENIA with $k = 1, 2, 3$ over MMSE-SE3 are 2.3dB, 3.4dB and 3.5dB respectively. Furthermore, the performance of MMSE-SENIA improves rapidly with k and is almost indistinguishable for $k = 2, 3$ from that of MMSE-EMI. In the 128×16 MIMO system, when BER $\geq 7.85 \times 10^{-5}$, MMSE-SENIA with $k = 2, 3$ has indistinguishable performance from MMSE-EMI, and is aproximately 0.6dB and 0.2dB worse than MMSE-EMI at BER $= 5.14 \times 10^{-6}$. In the 32×4 MIMO system, MMSE-SENIA with $k = 2, 3$ is indistinguishable from MMSE-EMI when BER $\geq 1.32 \times 10^{-4}$, and exhibits only 0.6dB and 0.2dB performance losses at BER $= 1.24 \times 10^{-5}$. In addition, from Fig.1, we see the error floors when SNR $\geq$ 14dB for MMSE-SE3 and MMSE-SENIA1, caused by the residual estimation error of (26). With MMSE-SE3 the error floor occurs at BER $= 1.6 \times 10^{-4}$, while with MMSE-SENIA1 the error floor occurs at BER $= 7 \times 10^{-5}$. For MMSE-SENIA2/3, no error floors are observed for BER $\geq 10^{-6}$.

In Fig. 2, we present the BER performance of MMSE detectors exploiting K-SENIA-IU in 128×32 and 32×10 16-QAM MIMO systems, where the system loading factor α exceeds the convergence constraint. The MMSE detectors employing K-SENIA-IU with size of initial approximate matrix inverse N_i and k iterations of K-SENIA, are referred to as MMSE-SENIAk-IU ($N_t = N_i + (N_t - N_i)$). We also consider MMSE-EMI, MMSE-SE3, MMSE-SENIAk and MMSE that exploits SE3-IU, referred to as

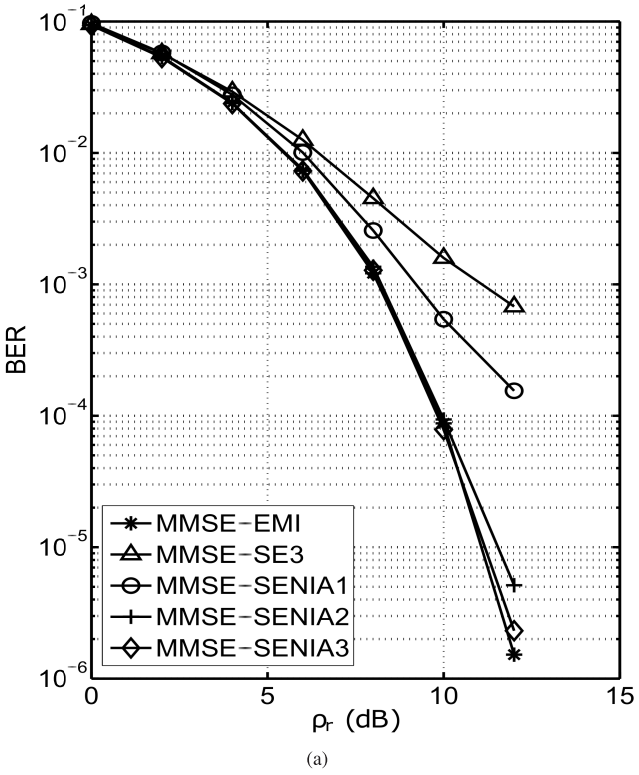

(a)

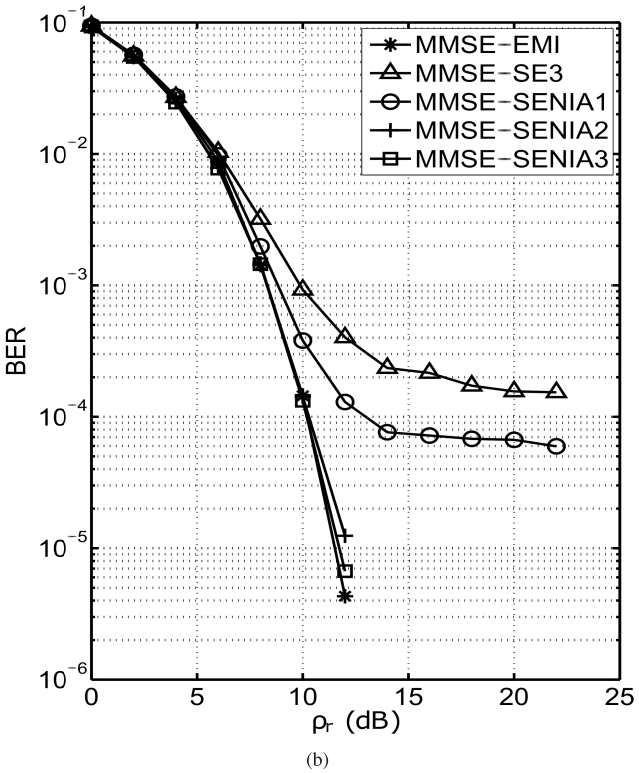

(b)

FIGURE 1. BER performance of MMSE-SENIA in (a) 128 × 16 MIMO and (b) 32 × 4 16-QAM MIMO systems.

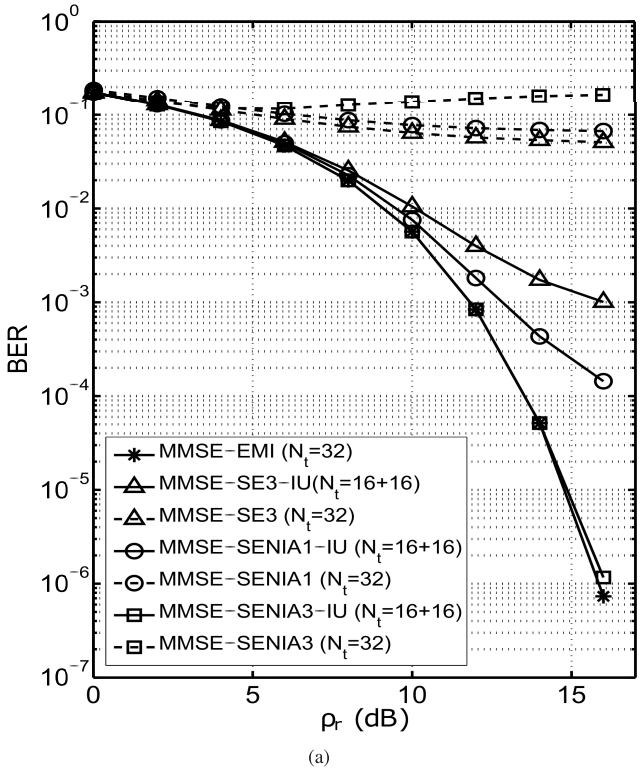

(a)

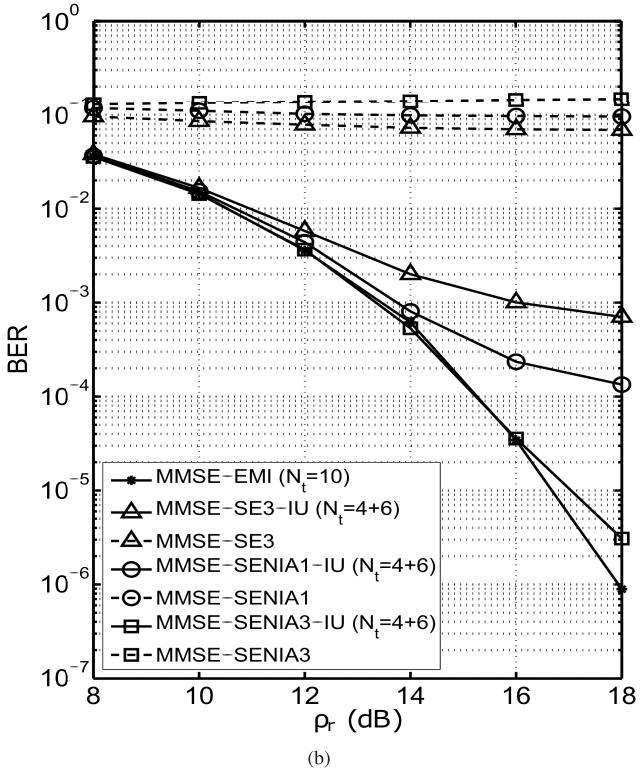

(b)

FIGURE 2. BER performance of MMSE-SENIA-IU in (a) 128 × 32 MIMO and (b) 32 × 10 16-QAM MIMO systems.

MMSE-SE3-IU ($N_t = N_i + (N_t - N_i)$), in which the initial approximate matrix inverse is computed by 3-term SE. We observe from Fig. 2 that because of higher system loading factors, MMSE-SE3 and MMSE-SENIA with $k = 1, 3$ fail to converge to the exact matrix inverse, as demonstrated by the BER not decreasing when ρ_s increases. However,

MMSE-SENIA-IU with $k = 3$ can achieve almost indistinguishable performance from MMSE-EMI. In the 128×32 MIMO system, MMSE-SENIA3-IU performs indistinguishable from MMSE-EMI when BER $\geq 5.14 \times 10^{-5}$ and is 0.2dB worse at BER $= 1.17 \times 10^{-6}$. In the 32×10 MIMO system, when BER $\geq 3.58 \times 10^{-5}$, the performance of MMSE-SENIA3-IU is indistinguishable from MMSE-EMI and exhibits only 0.7dB loss at BER $= 3.08 \times 10^{-6}$. These results demonstrate the capability of K-SENIA-IU to provide good performance at BER ranges of practical interest in higher loaded LS-MIMO systems. Next we show how such approximate matrix inversion technique can be integrated into selection list detection for LS-MIMO systems.

III. SELECTION BASED LIST DETECTION FOR LARGE-SCALE MIMO

A. GENERAL STRUCTURE OF SELECTION BASED LIST DETECTOR

At the receiver, a frame error (detection error) occurs if there is at least one error in the estimated symbol vector. For the MIMO system of (1) the optimal detector (in the sense of lowest average detection error probability) when $\mathbf{H}$ is known, is the maximum likelihood detector (MLD), employing the minimum Euclidean distance (MED) rule [6]

$$\hat{\mathbf{s}}^{ML} = \arg \min_{\hat{\mathbf{s}} \in \mathbb{A}^{N_t}} ||\mathbf{y} - \mathbf{H}\hat{\mathbf{s}}||^2, \tag{27}$$

where $||\cdot||$ denotes the Euclidean norm. Consider an alternative representation of MLD in (27). Let $\mathbf{H}_1 \in \mathbb{C}^{N_r \times N}$ denote a sub-matrix composed of N columns from $\mathbf{H}$, where $1 \leq N \leq N_t$, and let $\mathbf{s}_1 \in \mathbb{C}^{N \times 1}$ denote the symbol sub-vector whose components are transmitted over the channel corresponding to $\mathbf{H}_1$. Similarly, let $\mathbf{H}_2 \in \mathbb{C}^{N_r \times (N_t - N)}$ denote the sub-matrix composed of the remaining columns from $\mathbf{H}$ and $\mathbf{s}_2 \in \mathbb{C}^{(N_t - N) \times 1}$ denote the symbol sub-vector whose components are transmitted over the channel corresponding to $\mathbf{H}_2$. Thus (1) can be rewritten as

$$\mathbf{y} = \mathbf{H}_1\mathbf{s}_1 + \mathbf{H}_2\mathbf{s}_2 + \mathbf{n}. \tag{28}$$

Let $\hat{\mathbf{s}}_1, \hat{\mathbf{s}}_2$ denote the estimates of $\mathbf{s}_1, \mathbf{s}_2$. Let $[\hat{\mathbf{s}}_1^1, \hat{\mathbf{s}}_1^2, \ldots \hat{\mathbf{s}}_1^K]$, $K = M^N$ denote all the possible values of $\hat{\mathbf{s}}_1$, and $[\hat{\mathbf{s}}_2^1, \hat{\mathbf{s}}_2^2, \ldots, \hat{\mathbf{s}}_2^Q]$, $Q = M^{N_t - N}$ denote all the possible values of $\hat{\mathbf{s}}_2$. Then the ML solution of (27) can be rewritten as

$$(\hat{\mathbf{s}}^{ML})^T = [(\hat{\mathbf{s}}_1^{ML})^T, (\hat{\mathbf{s}}_2^{ML})^T] \text{ where } \hat{\mathbf{s}}_1^{ML} = \hat{\mathbf{s}}_1^{\tilde{k}}, \quad \hat{\mathbf{s}}_2^{ML} = \hat{\mathbf{s}}_2^{\tilde{q}}, \tag{29}$$

and

$$[\tilde{k}, \tilde{q}] = \arg \min_{k \in [1,2 \ldots K]} \min_{q \in [1,2,\ldots,Q]} ||\mathbf{y} - \mathbf{H}_1\hat{\mathbf{s}}_1^k - \mathbf{H}_2\hat{\mathbf{s}}_2^q||^2. \tag{30}$$

This equivalent representation of the MLD can be divided into three steps. First consider all the possible sub-vector hypotheses $\hat{\mathbf{s}}_1^k$ of $\mathbf{s}_1$, and obtain the residual observations

$$\mathbf{y}^k = \mathbf{y} - \mathbf{H}_1\hat{\mathbf{s}}_1^k, \quad k = 1, 2, \ldots, K. \tag{31}$$

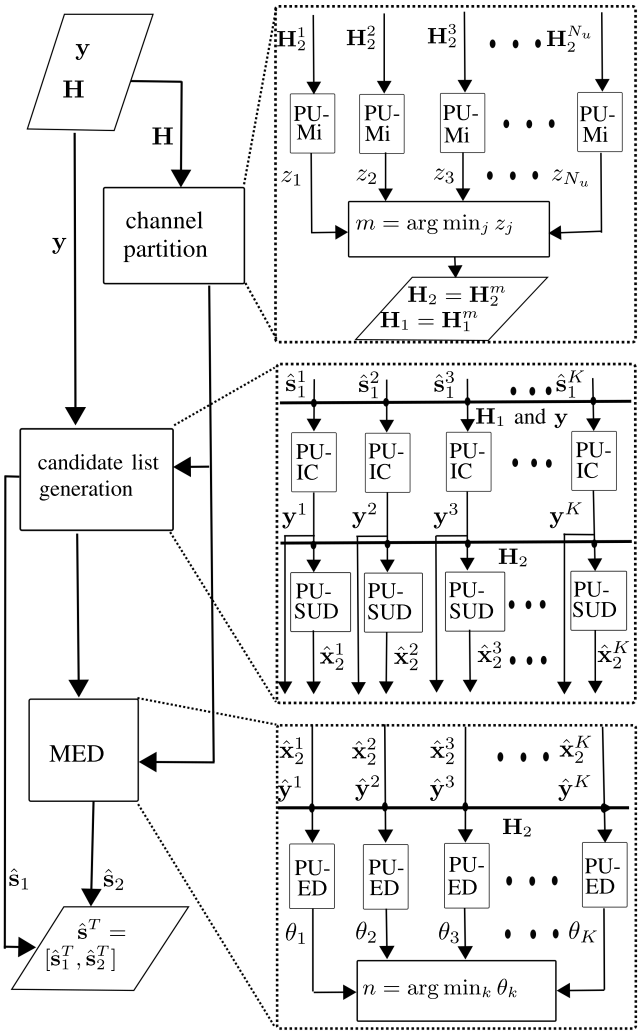

FIGURE 3. Block diagram of Selection Based List Detector with DMS channel partition and V-BLAST-SIC sub-detection.

Then solve

$$\hat{\mathbf{x}}_2^k = \arg \min_{\tilde{\mathbf{s}}_2 \in [\hat{\mathbf{s}}_2^1, \hat{\mathbf{s}}_2^2 \ldots, \hat{\mathbf{s}}_2^Q]} ||\mathbf{y}^k - \mathbf{H}_2\tilde{\mathbf{s}}_2||^2, \quad k = 1, 2, \ldots, K \tag{32}$$

$$\tilde{k} = \arg \min_{k \in [1,2,\ldots,K]} ||\mathbf{y}^k - \mathbf{H}_2\hat{\mathbf{x}}_2^k||^2, \tag{33}$$

Finally we have $\hat{\mathbf{s}}_1^{ML} = \hat{\mathbf{s}}_1^{\tilde{k}}, \hat{\mathbf{s}}_2^{ML} = \hat{\mathbf{x}}_2^{\tilde{k}}$.

This selection based list detection technique [27] first generates a list of candidates for possible transmitted symbol vectors estimates $\hat{\mathbf{s}}^k, k = 1, 2, \cdots, M^N$, then selects the best candidate in the list using the MED rule as the final decision. In Fig. 3 we illustrate the structure of this selection based list detection algorithm with DMS channel partition and V-BLAST ordered MMSE-SIC (V-BLAST-SIC) [49] sub-detector. The structure of Fig. 3, consists of three parallelizable stages:

- Channel Partition: The sub-matrices $\mathbf{H}_1$ and $\mathbf{H}_2$ in (30) are first obtained based on the channel partition rule.

The DMS rule [50] chooses the subset of the columns of $\mathbf{H}$ with the strongest weakest data substream (in the sense of postprocessing SINR using MMSE criterion [51]) and forms $\mathbf{H}_2$. Define the possible subsets $\mathbf{H}_2^j, j = 1, 2, \cdots, N_u$, where $N_u = \binom{N_t}{N}$. The subset chosen by DMS rule $\mathbf{H}_2^m$ is given by

$$m = \arg \min_{j=1,2,\cdots,N_u} z_j \tag{34}$$

$$z_j = \max_{k=1,2,\cdots,N_t-N} [((\mathbf{H}_2^j)^H \mathbf{H}_2^j + \rho_s \mathbf{I})^{-1}]_{kk} \tag{35}$$

The parallel structure of this procedure is shown in Fig. 3. In the first phase, the matrix inversions in (35) are computed by the processing units (PU) of matrix inversion (Mi) in parallel, in which the fast K-SENIA-IU can be used instead of exact matrix inversion. Then in the second phase, the subset is chosen based on (34).

- Candidate list generation: Use (31) to obtain K residual observations $\mathbf{y}^k$, then instead of performing an exhaustive search in (32), V-BLAST-SIC [27] is employed to obtain the estimates $\hat{\mathbf{x}}_2^k, k = 1, 2, \ldots, K$. As shown in Fig. 3, interference cancellations and V-BLAST-SIC are performed in parallel by the PU of interference cancellation (IC) and PU of sub-detector (SUD) respectively. The number of parallel pipelines required is M^N. The inverse $(\mathbf{H}_2^H \mathbf{H}_2 + \rho_s \mathbf{I})^{-1}$ required by V-BLAST-SIC is already computed at the channel partition stage.
- Final decison: Based on the MED decision rule of (33), the Euclidean distance (ED) of all M^N symbol vector candidates in the list are computed by the PU of ED, and the best candidate is selected as the final decision.

The sufficient condition for the selection based list algorithm with DMS channel partition and V-BLAST-SIC sub-detector to achieve optimal asymptotic diversity N_r is [27]

$$N = N_{min} = \lceil \sqrt{\frac{(N_r - N_t)^2}{4} + N_r} - \frac{(N_r - N_t)}{2} - 1 \rceil, \tag{36}$$

where $\lceil x \rceil$ denote the minimum integer no less than x.

B. IMPACT OF CHANNEL HARDENING ON CHANNEL PARTITION AND V-BLAST ORDERING

The DMS and V-BLAST ordering rules both use the postprocessing SINR of MMSE criterion [51] as a reliability measure of the symbol sub-datastreams. For the kth estimate of MMSE detection, the postprocessing SINR γ_k is [41], [52]

$$\gamma_k = \frac{\rho_s}{[(\mathbf{H}^H \mathbf{H} + \rho_s^{-1} \mathbf{I})^{-1}]_{kk}} - 1 = \frac{1}{1 - \mathbf{h}_k \mathbf{R}_y^{-1} \mathbf{h}_k} - 1, \tag{37}$$

where $\mathbf{R}_y = (\mathbf{H}\mathbf{H}^H + \rho_s^{-1}\mathbf{I})$ is the autocorrelation matrix of $\mathbf{y}$. The V-BLAST-SIC algorithm [49] evaluates at each layer the reliabilities of the symbol sub-datastreams in the sense of postprocessing SINR, and detects the one with the strongest postprocessing SINR. Then, the interference from the detected symbol is cancelled from the received signal vector. Let $[\mathbf{A}]_k$ denote the kth row of $\mathbf{A}$, the V-BLAST-SIC procedure is given by Algorithm 2.

Algorithm 2 V-BLAST-SIC

procedure ($\mathbf{H}$, $\mathbf{y}$)
  $\mathbf{B}^{(0)} = \mathbf{H}$, $\mathbf{y}^{(0)} = \mathbf{y}$
  for $i = 1 \rightarrow N_t$ **do**
    $\phi^i = \arg \min_{k=1,2,\cdots,N_t-i+1} [(\mathbf{W}^{-1})^{(i)}]_{kk}$ ▷ find the index of the sub-datastream with the strongest postprocessing SINR, where $(\mathbf{W}^{-1})^{(i)} = [(\mathbf{B}^{(i-1)})^H \mathbf{B}^{(i-1)} + \rho_s^{-1}\mathbf{I}]^{-1}$
    $\mathbf{g}_{MMSE} = [(\mathbf{W}^{-1})^{(i)}]_{\phi^i} (\mathbf{B}^{i-1})^H$ ▷ compute the MMSE equalization vector
    $\hat{\mathbf{s}}_{\phi^i} = \mathcal{Q}[\mathbf{g}_{MMSE} \mathbf{y}^{(i-1)}]$ ▷ detect ϕ^ith symbol
    $\mathbf{y}^{(i)} = \mathbf{y}^{(i-1)} - \mathbf{h}_{\phi^i} \hat{\mathbf{s}}_{\phi^i}$ ▷ cancel the interference of the detected symbol from the received signal vector, where $\mathbf{h}_{\phi^i}$ is the ϕ^ith column of $\mathbf{H}$
    update $\mathbf{B}^{(i)}$ by removing $\mathbf{h}_{\phi^i}$ from $\mathbf{B}^{(i-1)}$
  end for
end procedure

A fast recursive implementation of V-BLAST-SIC can be found in [53]. Firstly, $(\mathbf{W}^{-1})^{(1)} = [(\mathbf{H}^H \mathbf{H} + \rho_s^{-1}\mathbf{I})]^{-1}$ is computed, then at ith ($i \geq 2$) layer, $(\mathbf{W}^{-1})^{(i)}$ is updated from $(\mathbf{W}^{-1})^{(i-1)}$ instead of being recomputed from scratch, so that only one matrix inversion is required in V-BLAST-SIC. The complexity of this implementation scales as $\mathbb{O}((N_t)^3)$.

Both DMS and V-BLAST ordering are effective if the reliabilities of the symbol sub-datastreams are highly diverse [50], [52]. In LS-MIMO, due to channel hardening (6), the diagonal elements of $((\mathbf{H}_2^j)^H \mathbf{H}_2^j + \rho_s^{-1}\mathbf{I})^{-1}$ in (35) and $((\mathbf{B}^{(i)})^H \mathbf{B}^{(i)} + \rho_s^{-1}\mathbf{I})^{-1}$ at each layer of V-BLAST-SIC become equal. Therefore, with $N_t, N_r \rightarrow \infty, \alpha \rightarrow 0$, the postprocessing SINR becomes ineffective as a reliability measure, rendering DMS and V-BLAST ordering perform as channel independent selection (CIS) and random ordering.

C. INTEGRATION OF K-SENIA/IU INTO SELECTION BASED LIST DETECTION AND BER PERFORMANCE

Although DMS and V-BLAST ordering perform as CIS and random ordering asymptotically (i.e. $N_r, N_t \rightarrow \infty$, $\alpha \rightarrow 0$), when the system size is not extremely large such orderings are still useful for performance improvement. Large matrix inversion is heavily used in the DMS channel partition stage, and the result is reused for candidate list generation as $(\mathbf{W}^{-1})^{(1)}$ in V-BLAST-SIC, where K-SENIA-IU can be employed to replace exact matrix inversion. The advantages of using K-SENIA-IU are twofold. As shown in section II-B, the large processing latency of exact matrix inversion may cause a delay exceeding the channel coherence time, while K-SENIA-IU provides much lower latency due to deeper parralelism in each PU-Mi in Fig. 3, and its hardware implementation is simpler.

The computer simulation setup that has been used for performance evaluation is detailed in Appendix B. We consider the impact of channel hardening on selection based list detection by comparing different channel partition schemes (DMS and CIS), different matrix inversion schemes (exact matrix inversion (Ei) and K-SENIA-IU (Ai)) and different ordering strategies of SIC (V-BLAST-SIC and SIC without ordering). The schemes considered are CIS-Ai-SIC, CIS-Ai-VBLAST-SIC, DMS-Ai-SIC, DMS-Ai-VBLAST-SIC and DMS-Ei-VBLAST-SIC.

In Fig. 4 we present results for 128×32 and 128×96 4QAM MIMO systems (i.e. system loading factor $\alpha = 0.25$ and 0.75), where the number of antenna selected at channel partition stage is $N = 1$, the number of iterations of K-SENIA is 3 and the initial size of matrix inverse for IU N_{ini} is 16. It can be observed that both system configurations of DMS-Ai-VBLAST-SIC have almost indistinguishable performance from DMS-Ei-VBLAST-SIC and no error floor is observed for BER $\geq 10^{-6}$. This demonstrates the suitability of K-SENIA-IU for selection based list detectors. Then, by comparing CIS-Ai-SIC with DMS-Ai-SIC, and CIS-Ai-VBLAST-SIC with DMS-Ai-VBLAST-SIC, we can conclude that in LS-MIMO, when N is small, the channel partition scheme has a very small impact on performance. The ordering strategy, however, has a larger impact on performance. For example, in Fig. 4(a), CIS-Ai-VBLAST-SIC performs about 0.4dB better than CIS-Ai-SIC at BER $= 2.86 \times 10^{-6}$, and in Fig. 4(b), the SNR gain of CIS-Ai-VBLAST-SIC over CIS-Ai-SIC is about 1.1dB at BER $= 1.60 \times 10^{-5}$. Therefore, hereinafter, we use CIS for channel partition in large systems, so that the computational complexity required by the DMS of (34) and (35) (i.e., the computation of $N_u = \binom{N_t}{N}$ matrix inversions) can be avoided with negligible performance loss.

In Fig. 5 we consider the effect of N on CIS-Ai-SIC and CIS-Ai-VBLAST-SIC in a 128×96 4-QAM MIMO system. We can see that in LS-MIMO with CIS-Ai-SIC and CIS-Ai-VBLAST-SIC increasing N from 1 to 2 provides very limited performance gains.

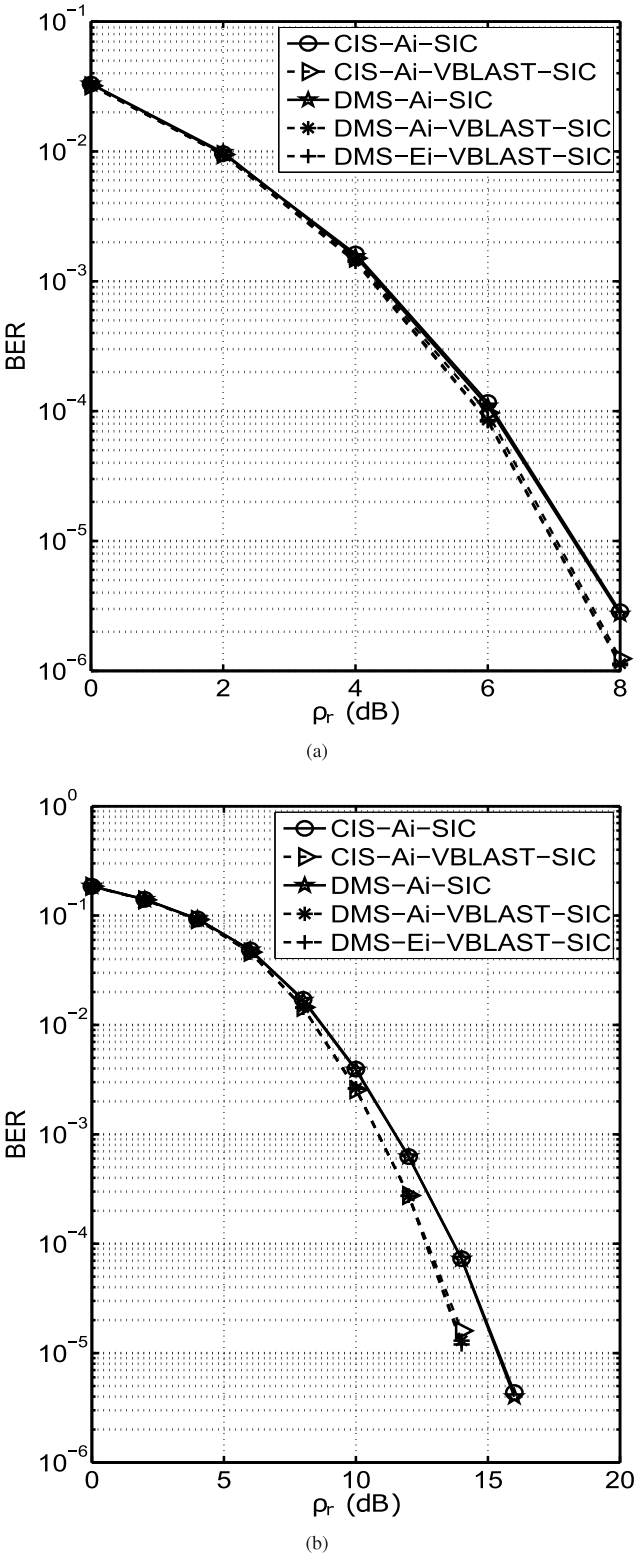

FIGURE 4. BER performance of selection based list detections in (a) 128 × 32 MIMO and (b) 128 × 96 4-QAM MIMO systems with $N = 1$.

IV. SELECTION BASED LIST DETECTION WITH IMPROVED OSIC SUB-DETECTION

A. IMPROVED ORDERING FOR SIC SUB-DETECTORS

From Section III we see that in LS-MIMO with selection based list detection, the ordering scheme of sub-detectors affects performance more significantly than the channel partition strategy. We also see that V-BLAST ordering becomes less effective due to channel hardening. Hence, to improve performance we consider improved ordering (IO) based on the simplified Maximum a Posterior (MAP) log ratio of the decision bit and Gaussian approximation of MMSE soft estimate $\tilde{\mathbf{s}} = \mathbf{G}_{MMSE}\mathbf{y}$ [41], namely Type-L reliability. For modulation schemes with multiple bits per symbol, the Type-L reliability of the kth decision symbol is [41]

$$L_k = (1 + \gamma_k)(|\Re(\tilde{\mathbf{s}}_k)| + |\Im(\tilde{\mathbf{s}}_k)|), \quad k = 1, 2, \cdots, N_t, \tag{38}$$

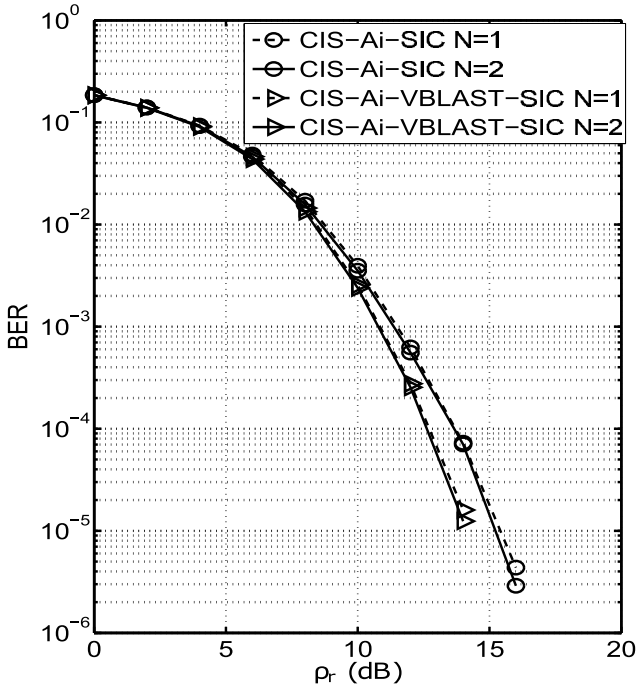

FIGURE 5. BER performance of CIS-Ai-SIC/VBLAST-SIC with different N in a 128 × 96 4-QAM MIMO system.

where $\Re(\cdot)$ and $\Im(\cdot)$ denote the real and imaginary parts. Using (37) in (38) and removing the multiplicative constant ρ_s yields

$$L_k \triangleq \frac{|\Re(\tilde{\mathbf{s}}_k)| + |\Im(\tilde{\mathbf{s}}_k)|}{[(\mathbf{H}^H\mathbf{H} + \rho_s^{-1}\mathbf{I})^{-1}]_{kk}}, \quad k = 1, 2, \cdots, N_t \quad (39)$$

The Type-L reliability measure takes into account postprocessing SINR and the magnitude of $\tilde{\mathbf{s}}_k$. The detection order with improved ordering SIC (IO-SIC) is also influenced by the residual observations $\mathbf{y}^k$ of (31), and with IO-SIC as the sub-detector it can provide more diverse candidate symbol vectors in the list. Type-L reliabilities are formed for the undetected symbol sub-datastreams and the most reliable sub-datastream selected is quantized for hard decisions. The procedure employing IO-SIC is summarized in Algorithm 3.

We can see from Algorithm 3, that at the ith layer of IO-SIC, the soft estimates of undetected symbol sub-datastreams are required in order to evaluate their Type-L reliabilities, in which the computation of the estimate $(\mathbf{B}^{(i-1)})^H\mathbf{y}^{(i-1)}$ has a complexity that scales as $\mathbb{O}((N_t - i + 1)^2)$. Next, we show that this estimate can be updated from the one of the previous layer with lower complexity. To elaborate further, given the estimate at the ith layer

$$[(\mathbf{B}^{(i-1)})^H\mathbf{y}^{(i-1)}]^T = [\mathbf{h}_1^H\mathbf{y}^{(i-1)}, \mathbf{h}_2^H\mathbf{y}^{(i-1)}, \cdots, \mathbf{h}_{\phi^i}^H\mathbf{y}^{(i-1)}, \cdots, \mathbf{h}_{N_t-i+1}^H\mathbf{y}^{(i-1)}]^T, \quad (40)$$

where ϕ^i is the index of the most reliable sub-datastream that is chosen to be detected at the ith layer, then at the $i+1$ layer,

Algorithm 3 IO-SIC

procedure ($\mathbf{H}$, $\mathbf{y}$)
  $\mathbf{B}^{(0)} = \mathbf{H}$, $\mathbf{y}^{(0)} = \mathbf{y}$
  for $i = 1 \to N_t$ **do**
    $\tilde{\mathbf{s}}^{(i)} = (\mathbf{W}^{-1})^{(i)}(\mathbf{B}^{(i-1)})^H\mathbf{y}^{(i-1)}$ ▷ Obtain the soft estimates of the undetected symbol sub-datastreams, where $(\mathbf{W}^{-1})^{(i)} = (\mathbf{B}^{(i-1)})^H\mathbf{B}^{(i-1)} + \rho_s^{-1}\mathbf{I}$
    for $j = 1 \to N_t - i + 1$ **do**
      $L_j = \frac{|\Re(\tilde{\mathbf{s}}_k^{(i)})| + |\Im(\tilde{\mathbf{s}}_k^{(i)})|}{[(\mathbf{W}^{(i)})^{-1}]_{kk}}$ ▷ compute Type-L reliabilities of undetected symbol sub-datastreams
    end for
    $\phi^i = \arg\max_{j=1,2,\cdots,N_t-i+1} L_j$ ▷ find the index of the most reliable sub-datastream
    $\hat{\mathbf{s}}_{\phi^i} = \mathcal{Q}[\tilde{\mathbf{s}}_{\phi^i}^{(i)}]$ ▷ Quantize ϕ^ith component of $\tilde{\mathbf{s}}^{(i)}$
    $\mathbf{y}^{(i)} = \mathbf{y}^{(i-1)} - \mathbf{h}_{\phi^i}\hat{\mathbf{s}}_{\phi^i}$ ▷ cancel the interference of the detected symbol from the received signal vector, where $\mathbf{h}_{\phi^i}$ is the ϕ^ith column of $\mathbf{H}$
    update $\mathbf{B}^{(i)}$ by removing $\mathbf{h}_{\phi^i}$ from $\mathbf{B}^{(i-1)}$
  end for
end procedure

using $\mathbf{y}^{(i)} = \mathbf{y}^{i-1} - \mathbf{h}_{\phi^i}\hat{\mathbf{s}}_{\phi^i}$, we have

$$(\mathbf{B}^{(i)})^H\mathbf{y}^{(i)} = \begin{bmatrix} \mathbf{h}_1^H\mathbf{y}^{(i)} \\ \mathbf{h}_2^H\mathbf{y}^{(i)} \\ \vdots \\ \mathbf{h}_{\phi^i-1}^H\mathbf{y}^{(i)} \\ \mathbf{h}_{\phi^i+1}^H\mathbf{y}^{(i)} \\ \vdots \\ \mathbf{h}_{N_t-i}^H\mathbf{y}^{(i)} \end{bmatrix} = \begin{bmatrix} \mathbf{h}_1^H\mathbf{y}^{(i-1)} \\ \mathbf{h}_2^H\mathbf{y}^{(i-1)} \\ \vdots \\ \mathbf{h}_{\phi^i-1}^H\mathbf{y}^{(i-1)} \\ \mathbf{h}_{\phi^i+1}^H\mathbf{y}^{(i-1)} \\ \vdots \\ \mathbf{h}_{N_t-i}^H\mathbf{y}^{(i-1)} \end{bmatrix} - \begin{bmatrix} \mathbf{h}_1^H\mathbf{h}_{\phi^i}\hat{\mathbf{s}}_{\phi^i} \\ \mathbf{h}_2^H\mathbf{h}_{\phi^i}\hat{\mathbf{s}}_{\phi^i} \\ \vdots \\ \mathbf{h}_{\phi^i-1}^H\mathbf{h}_{\phi^i}\hat{\mathbf{s}}_{\phi^i} \\ \mathbf{h}_{\phi^i+1}^H\mathbf{h}_{\phi^i}\hat{\mathbf{s}}_{\phi^i} \\ \vdots \\ \mathbf{h}_{N_t-i}^H\mathbf{h}_{\phi^i}\hat{\mathbf{s}}_{\phi^i} \end{bmatrix} \quad (41)$$

where the first term of (41) can be obtained from (40), and $\mathbf{h}_k^H\mathbf{h}_{\phi^i}, k, \phi^i = 1, 2, \cdots, N_t$ in the second term are the components of $\mathbf{H}^H\mathbf{H}$ which are already obtained for computing $\mathbf{W} = \mathbf{H}^H\mathbf{H} + \rho_s^{-1}\mathbf{I}$. Hence there is no extra overhead for obtaining (41) and the complexity required for computing $(\mathbf{B}^{(i)})^H\mathbf{y}^{(i)}$ is that of a vector subtraction, that scales as $\mathbb{O}(N_t - i + 1)$. Similar to the fast implementation of V-BLAST-SIC [53], in IO-SIC only $(\mathbf{W}^{-1})^{(1)}$ at the first layer is required to be computed. Then $(\mathbf{W}^{-1})^{(i)}$ at $i \geq 2$ layers can be updated with low complexity, and $(\mathbf{W}^{-1})^{(1)}$ can be approximated by K-SENIA/IU.

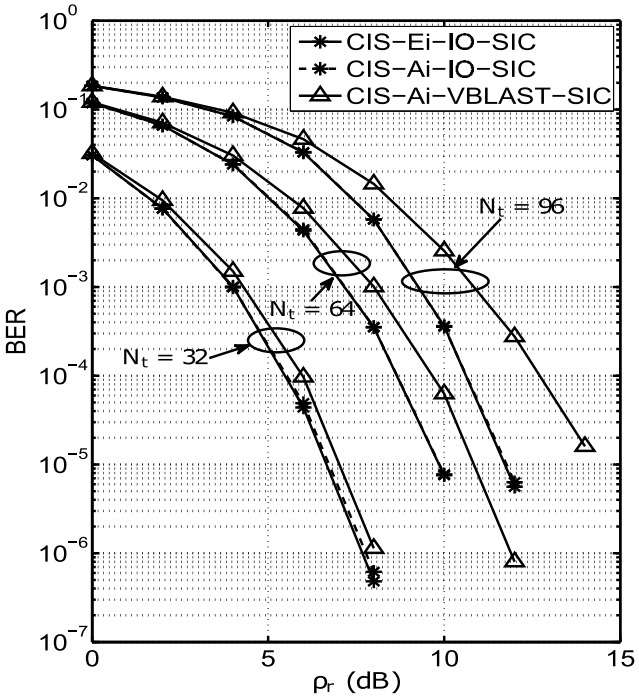

FIGURE 6. BER performance of IO-SIC for $N_r = 128$, $N_t = 32, 64, 96$ with 4-QAM in MIMO systems with $N = 1$.

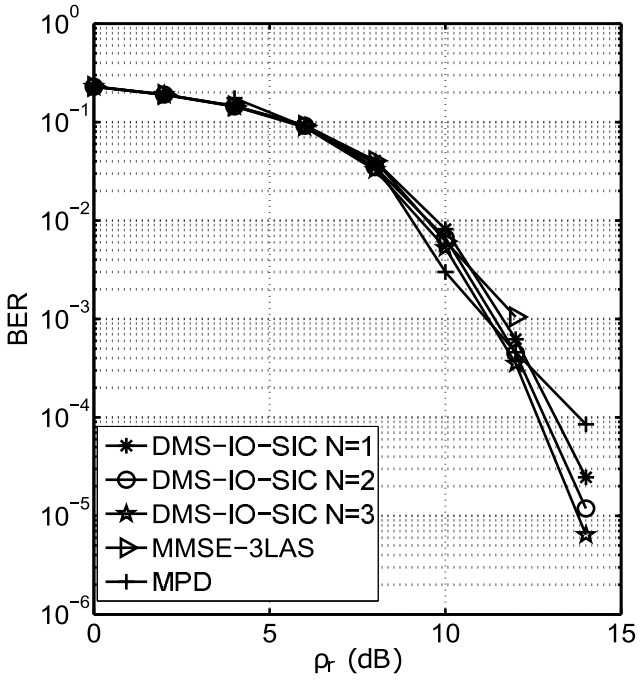

FIGURE 7. BER performance of DMS-IO-SIC, MMSE-3LAS and MPD (data for MMSE-3LAS and MPD collected from [42] and [22]) for 32 × 32 4-QAM MIMO.

B. BER PERFORMANCE OF IO-SIC IN LS-MIMO SYSTEMS

Next we present simulation results for BER performance of selection based list detection with CIS channel partition and IO-SIC sub-detection. The setup for computer simulations is detailed in Appendix B. For comparison, selection based list detection that uses V-BLAST-SIC for sub-detection is also considered. Furthermore, we consider exact matrix inversion (Ei) as well as K-SENIA/IU (Ai), and hence the schemes considered in this subsection are referred to as CIS-(Ei/Ai)-(IO/VBLAST)-SIC.

In Fig. 6 we present BER results for LS-MIMO 4-QAM systems with fixed number of BS antennas $N_r = 128$ and varying number of single antenna users $N_t = 32, 64, 96$, corresponding to system loading factors $\alpha = 0.25, 0.5, 0.75$. The number of antennas selected at the channel partition stage is $N = 1$, for K-SENIA-IU the number of iterations of K-SENIA is 3, and the initial size of the matrix inversion of IU is 16. It is observed that CIS-Ai-IO-SIC performs indistinguishably from CIS-Ei-IO-SIC at BER $\geq 10^{-6}$ in all the system configurations, demonstrating the effectiveness of K-SENIA-IU in selection based list detections with IO-SIC. Furthermore, in all the system configurations, CIS-Ei-IO-SIC outperforms CIS-Ei-VBLAST-SIC and the performance gain increases when the system loading factor increases. For example, in the 128 × 32 system at BER $= 1.14 \times 10^{-6}$ the performance gain achieved by CIS-Ei-IO-SIC over CIS-Ai-VBLAST-SIC is about 0.4dB, in the 128 × 64 system at BER $= 7.57 \times 10^{-6}$ CIS-Ei-IO-SIC is about 1dB better than CIS-Ai-VBLAST-SIC, and in the 128 × 96 system CIS-Ei-IO-SIC achieves about 2.5dB SNR gain over CIS-Ai-VBLAST-SIC at BER $= 1.60 \times 10^{-5}$. The performance gain of selection based list detections with IO-SIC over that with V-BLAST-SIC improves in the higher loaded systems because the Type-L reliability measure converges to the optimum MAP-based reliability measure with increasing number of users [41].

V. PERFORMANCE AND COMPLEXITY COMPARISON

This section presents a comparison, including performance, complexity and structure, between the proposed selection based list algorithm of section III-C referred to as DMS/CIS-IO-SIC, and two state-of-art LS-MIMO detection schemes, namely multistage LAS algorithm [15], [42] and MPD [22].

A. BER PERFORMANCE COMPARISON

In Fig. 7 we present the results for DMS-IO-SIC with different number of antennas selected at channel partition stage ($N = 1, 2, 3$), multistage LAS algorithm named MMSE-3LAS, and the MPD algorithm for a 32 × 32 4-QAM MIMO system. The reason of using DMS in such a system is that in medium size MIMO, it is still more effective than CIS. It can be observed that all DMS-IO-SIC configurations outperform MMSE-3LAS. For example, at BER $= 1.05 \times 10^{-3}$, DMS-IO-SIC ($N = 1, 2, 3$) can achieve 0.4dB 0.65dB and 0.8dB SNR gain over MMSE-3LAS respectively, and MPD is about 1.4dB worse than DMS-IO-SIC ($N = 3$) at BER $= 8.50 \times 10^{-5}$. In such medium size MIMO systems, there is a noticeable performance improvement for DMS-IO-SIC when N increases. For example, at BER $= 2.46 \times 10^{-5}$, DMS-IO-SIC with $N = 3$ achieves about 0.7dB SNR gain over that of $N = 1$.

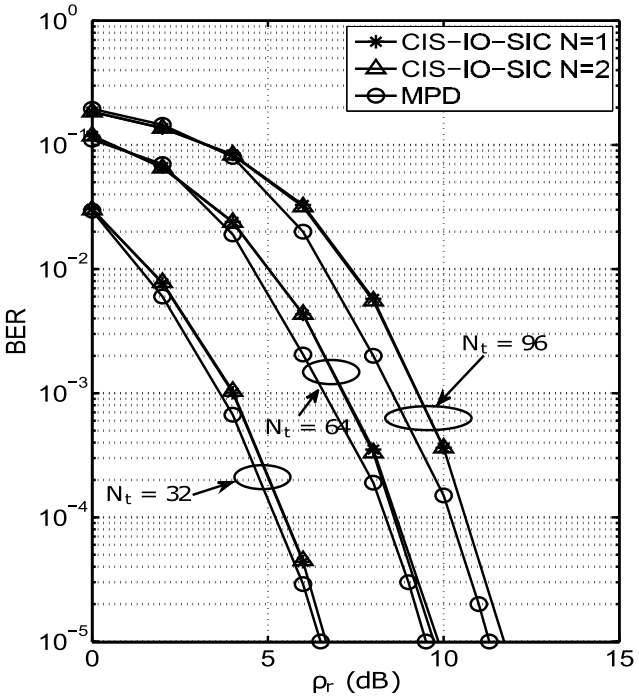

FIGURE 8. BER performance of CIS-IO-SIC and MPD (data for MPD collected from [22]) for $N_r = 128$, $N_t = 32, 64, 96$ 4-QAM MIMO.

In Fig. 8 we present the results of CIS-IO-SIC ($N = 1, 2$) as well as MPD for $N_r = 128$ and $N_t = 32, 64, 96$ with 4-QAM. With all system configurations, for BER $\geq 10^{-5}$, CIS-IO-SIC with $N = 1$ exhibits almost no performance loss compared with CIS-IO-SIC with $N = 2$, while the list size of the former is only $\frac{1}{4}$ of the latter. For all the system configurations considered, the performance loss of CIS-IO-SIC $N = 1, 2$ compared with MPD is just a fraction of dB. For example, in the 128×32 system, at BER $= 4.60 \times 10^{-5}$ CIS-IO-SIC is about 0.3dB worse than MPD, in the 128×64 system MPD is about 0.25dB better than CIS-IO-SIC at BER $= 3.0 \times 10^{-5}$, and in the 128×96 system at BER $= 2.0 \times 10^{-5}$ CIS-IO-SIC is about 0.4dB worse than MPD. In large size MIMO systems, a small list is enough to provide a competitive performance for CIS-IO-SIC.

B. COMPLEXITY ISSUES AND COMPARISON

For selection based list detection, assume the number of antenna selected at the channel partition stage is N. If CIS is used, then there is no complexity overhead at the channel partition stage. At the candidate list generation stage, computation of each residual $\mathbf{y}^k$ in (31) requires a complexity of order $\mathbb{O}(N_r N)$ for each sub-detector. Then consider each IO-SIC sub-detector. As seen in Algorithm 3, at the first layer, computation of $(\mathbf{W}^{-1})^{(1)}$ is required, where the use of exact matrix inversion requires a complexity of order $\mathbb{O}((N_t - N)^3)$ and the use of K-SENIA-IU, based on the analysis in section II-B, requires a complexity of order $\mathbb{O}(N_r(N_t - N)^2)$. Computation of the initial soft estimate $(\mathbf{B}^0)^H\mathbf{y}^0$ requires a complexity of order $\mathbb{O}(N_r(N_t - N))$. Then for the ith layer ($i \geq 2$), $(\mathbf{W}^{-1})^{(i)}$ can be updated based on the fast implementation in [53], which has a complexity that scales as $\mathbb{O}((N_t - N - i + 1)^2)$. The update of the soft estimate $(\mathbf{B}^{(i-1)})^H\mathbf{y}^{(i-1)}$ requires a complexity of order $\mathbb{O}(N_t - N - i + 1)$, and obtaining $\tilde{\mathbf{s}}^{(i)}$ has a complexity of order $\mathbb{O}((N_t - N - i + 1)^2)$. Finally the computation of Type-L reliabilities has a complexity that scales as $\mathbb{O}(N_t - N - i + 1)$, and calculation of $\mathbf{y}^{(i)} = \mathbf{y}^{(i-1)} - \mathbf{h}_{\phi^i}\hat{\mathbf{s}}_{\phi^i}$ has a complexity of order $\mathbb{O}(N_r)$. Hence, the computational complexity of obtaining one candidate symbol vector in the list is of order

$$\mathbb{O}((N_t - N)^3) + \sum_{i=2}^{N_t - N} [\mathbb{O}((N_t - N - i + 1)^2)] = \mathbb{O}((N_t - N)^3) \quad \text{For Ei,} \tag{42}$$

$$\mathbb{O}(N_r(N_t - N)^2) + \sum_{i=2}^{N_t - N} [\mathbb{O}((N_t - N - i + 1)^2)] = \mathbb{O}(N_r(N_t - N)^2) \quad \text{For Ai.} \tag{43}$$

For generating a candidate list of size M^N, the complexity is $\mathbb{O}(M^N(N_t - N)^3)$ for Ei and $\mathbb{O}(M^N N_r(N_t - N)^2)$ for Ai. In the final decision step, each candidate $\mathbf{y}^k - \mathbf{H}_2\hat{\mathbf{x}}_2^k$ in (33) is already computed at the SIC step, and only an Euclidean norm is required with complexity $\mathbb{O}(N_r)$, resulting in total complexity of $\mathbb{O}(M^N N_r)$ for this step. In conclusion, the overall complexity of DMS-(Ei/Ai)-IO-SIC is $\mathbb{O}(M^N(N_t - N)^3)$ and $\mathbb{O}(M^N N_r(N_t - N)^2)$ respectively.

The multistage LAS algorithm aims at reducing a cost function through multi-stage updates of an initial solution. The MMSE-3LAS employs 1 to 3-symbol neighborhood updates as steps in each stage, with initial solution generated by a MMSE detector of complexity $\mathbb{O}(N_r N_t^2)$. The empirical complexity of LAS searching based on simulation [42] is $\mathbb{O}(N_t^2)$. Therefore the overall complexity of multistage LAS is $\mathbb{O}(N_t^3)$.

The MPD algorithm is an iterative procedure that works on a graphical model and updates all the sub-data streams in each iteration. The establishment of the graphical model requires the computation of $\mathbf{H}^H\mathbf{y}$ and $\mathbf{H}^H\mathbf{H}$, with complexities $\mathbb{O}(N_r N_t)$ and $\mathbb{O}(N_r N_t^2)$ respectively. Then for a square M-QAM constellations each iteration has a complexity of $\mathbb{O}(\sqrt{M}N_t^2)$, and with iteration time n_I the total complexity of the iterative update process is $\mathbb{O}(n_I\sqrt{M}N_t^2)$. Hence the overall complexity of MPD scales as $\mathbb{O}(N_r N_t^2)$.

The complexity scaling results from this subsection are summarized in Table 1. We include also the results from [23] and [29] that are related to the techniques considered in our paper. As we can see from Table 1, Linear MMSE, CIS-Ei-IO-SIC, CIS-Ai-IO-SIC, MMSE-3LAS and MMSE-GAIL are comparable in complexity scaling with N_t and N_r. The message passing techniques MPD and AMP-LS scale slower with N_t and N_r. However these schemes do not have structural parallelism properties that are inherent in selection based list detection techniques such as CIS-Ei-IO-SIC, CIS-Ai-IO-SIC and MMSE-GAIL. It could be a useful endeavour to integrate selection based techniques

TABLE 1. Complexity scalling comparison.

Scheme	Reference	Complexity Scalling
Linear MMSE	[15]	$\mathbb{O}(N_r N_t^2)$
CIS-Ei-IO-SIC	this paper	$\mathbb{O}(M^N (N_t - N)^3)$
CIS-Ai-IO-SIC	this paper	$\mathbb{O}(M^N N_r (N_t - N)^2)$
MMSE-3LAS	[15], [42]	$\mathbb{O}(N_r N_t^2)$
MPD	[22]	$\mathbb{O}(n_I \sqrt{M} N_t^2)$ including establishment of graphical model $\mathbb{O}(N_r N_t^2)$
Approx. MPD (AMP-LS)	[23]	$\mathbb{O}(20 N_r N_t)$
MMSE-GAIL	[29]	$\mathbb{O}(12 N_r N_t^2)$

as in our paper or as in [29] (termed grouping there) into message passing detection algorithms for inducing structural parallelism.

VI. CONCLUSIONS

In this paper, we first propose a fast approximate matrix inversion scheme K-SENIA/IU, which is suitable for integration into selection based list detectors for lower latency and deeper parallelism, making it attractive for applications in LS-MIMO systems. By studying the impacts of the channel hardening phenomenon on selection based list detection, we found that when the size of the system increases, the postprocessing SINR based DMS channel partition rule and V-BLAST ordering become less effective. We also showed that in LS-MIMO systems, ordering has a larger impact on performance than channel partition. Based on this result, we considered an improved ordering scheme for SIC subdetection, that takes into account both postprocessing SINR and the received signal vector. Simulation results corroborate that a significant performance gain can be achieved by selection based list detection with improved ordering-SIC over the selection based list algorithm with V-BLAST-SIC. Then we compare the selection based list algorithm employing improved ordering with two state-of-art LS-MIMO detection techniques, multistage LAS and MPD. Simulation results show that the selection based list algorithm with improved ordering performs better than multistage LAS and it is at most a fraction of dB worse than MPD. In a medium size system (32×32), with DMS-IO-SIC, increasing N from 1 to 3 results in an observable performance improvement. However, in large size systems $N_r = 128, N_t = 32, 64, 96$, DMS can be replaced by CIS and N can be chosen as 1 with almost no performance loss while lowering complexity compared with $N = 2$. The complexities of the proposed selection based list detection, linear MMSE, multistage LAS and MMSE-GAIL have the same order of magnitude. The complexity of MPD based algorithms is lower, however selection based list algorithms, such as those proposed in this paper and MMSE-GAIL of [29], have inherent parallelism properties that can provide an implementation advantage. Therefore, the proposed selection based list algorithm is a competitive candidate for practical LS-MIMO detection. While in this work we assume spatially uncorrelated channels that are perfectly known at the receiver, the derived algorithms can be applied also on spatially correlated channels, and also when the channels are not perfectly known at the receiver. The effects of such imperfections on performance could be a subject for a folowing up study.

APPENDIX A

Given

$$\epsilon = \mathbb{E}(||\hat{\mathbf{s}}^{MMSE} - \hat{\mathbf{s}}^{MMSE-SENIA}||^2) = \mathbb{E}(||\mathbf{W}_{\triangle}^{-1}\mathbf{H}^H\mathbf{y}||^2),$$

then the use of (24) yields

$$\epsilon = \mathbb{E}(||(\mathbf{D}^{-1}\mathbf{E})^{2^{k+1}}\mathbf{W}^{-1}\mathbf{H}^H\mathbf{y}||^2). \tag{44}$$

Let $\mathbf{F} = (\mathbf{D}^{-1}\mathbf{E})^{2^{k+1}}$ and $\mathbf{G} = \mathbf{W}^{-1}\mathbf{H}^H$. With $Tr(\mathbf{X})$ denoting the trace of matrix $\mathbf{X}$, then (44) can be rewritten as

$$\begin{aligned}\epsilon &= \mathbb{E}(||\mathbf{FGy}||^2) = \mathbb{E}[Tr(\mathbf{FGyy}^H\mathbf{G}^H\mathbf{F}^H)] \\ &= Tr\{\mathbb{E}(\mathbf{FGyy}^H\mathbf{G}^H\mathbf{F}^H)\},\end{aligned} \tag{45}$$

and with (1) in (45) we have

$$\begin{aligned}\epsilon &= Tr\{\mathbb{E}[\mathbf{FG}(\mathbf{Hs}+\mathbf{n})(\mathbf{s}^H\mathbf{H}^H + \mathbf{n}^H)\mathbf{G}^H\mathbf{F}^H]\} \\ &= Tr\{\mathbb{E}[\mathbf{FGHss}^H\mathbf{H}^H\mathbf{G}^H\mathbf{F}^H] + \mathbb{E}[\mathbf{FGnn}^H\mathbf{G}^H\mathbf{F}^H] \\ &\quad + \mathbb{E}[\mathbf{FGHsn}^H\mathbf{G}^H\mathbf{F}^H] + \mathbb{E}[\mathbf{FGns}^H\mathbf{H}^H\mathbf{G}^H\mathbf{F}^H]\} \\ &= Tr\{\mathbb{E}[\mathbf{ss}^H]\mathbb{E}[\mathbf{FGHH}^H\mathbf{G}^H\mathbf{F}^H] \\ &\quad + \mathbb{E}[\mathbf{nn}^H]\mathbb{E}[\mathbf{FGG}^H\mathbf{F}^H]\} \\ &= Tr\{E_s\mathbb{E}[\mathbf{FGHH}^H\mathbf{G}^H\mathbf{F}^H] + \sigma_o^2\mathbb{E}[\mathbf{FGG}^H\mathbf{F}^H]\} \\ &= E_s Tr\{\mathbb{E}[\mathbf{FGHH}^H\mathbf{G}^H\mathbf{F}^H] \\ &\quad + \rho_s^{-1}\mathbb{E}[\mathbf{FGG}^H\mathbf{F}^H]\}\end{aligned} \tag{46}$$

At high SNR ($\rho_s \to \infty$) the second summand of (46) vanishes, and $\lim_{\rho_s\to\infty}\epsilon = E_s Tr\{\mathbb{E}[\mathbf{FGHH}^H\mathbf{G}^H\mathbf{F}^H]\}$. Furthermore, since

$$\begin{aligned}\lim_{\rho_s\to\infty}\mathbf{G} &= \lim_{\rho_s\to\infty}\mathbf{W}^{-1}\mathbf{H}^H \\ &= \lim_{\rho_s\to\infty}(\mathbf{H}^H\mathbf{H} + \rho_s^{-1}\mathbf{I})^{-1}\mathbf{H}^H = (\mathbf{H}^H\mathbf{H})^{-1}\mathbf{H}^H\end{aligned} \tag{47}$$

we have

$$\begin{aligned}\lim_{\rho_s\to\infty}\epsilon &= E_s\mathbb{E}\{Tr[\mathbf{FF}^H]\} \\ &= E_s\mathbb{E}[||\mathbf{F}||_F^2] = E_s\mathbb{E}[||(\mathbf{D}^{-1}\mathbf{E})^{2^{k+1}}||_F^2],\end{aligned} \tag{48}$$

where $||\cdot||_F$ denotes the Frobenius norm.

APPENDIX B

We simulated uncoded complex LS-MIMO uplink multiuser systems, with rectangular M-QAM (4-QAM and 16-QAM) modulation and Gray labeling. For each receive SNR level, the BER was estimated based on a minimum of 10^5 independent channel realizations and a minimum of 300 symbol errors. In each channel realization, for each single antenna user, $n_c = \log_2(M)$ independent randomly generated bits were mapped to a complex symbol. Then N_t complex symbols were transmitted by single antenna users over randomly generated Rayleigh block fading channels. Each component

of the channel matrix was generated as a CSCG random variable with zero mean and unit variance. The received signal vector was contaminated by AWGN.

The software testbed was implemented in C, compiled by a GCC compiler version 4.9.2 on a 64 bit Debian (release 8.2) Linux system. The experiments were performed on two desktop computers, one consisting of a quad core Intel I5-4th generation CPU with 3.2GHz clock rate, and the other consisting of a six core Intel I7-5th generation CPU with 3.5GHz clock rate.

ACKNOWLEDGMENT

T. Chen was with the Department of Electrical and Computer Engineering, McGill University, Montreal, QC, Canada.

REFERENCES

[1] T. L. Marzetta, "Noncooperative cellular wireless with unlimited numbers of base station antennas," *IEEE Trans. Wireless Commun.*, vol. 9, no. 11, pp. 3590–3600, Nov. 2010.

[2] F. Rusek *et al.*, "Scaling up MIMO: Opportunities and challenges with very large arrays," *IEEE Signal Process. Mag.*, vol. 30, no. 1, pp. 40–60, Jan. 2013.

[3] S. Yang and L. Hanzo, "Fifty years of MIMO detection: The road to large-scale MIMOs," *IEEE Commun. Surveys Tuts.*, vol. 17, no. 4, pp. 1941–1988, 4th Quart., 2015.

[4] S. Yang, T. Lv, R. G. Maunder, and L. Hanzo, "Unified bit-based probabilistic data association aided MIMO detection for high-order QAM constellations," *IEEE Trans. Veh. Technol.*, vol. 60, no. 3, pp. 981–991, Mar. 2011.

[5] W. Yi and H. Leib, "OFDM symbol detection integrated with channel multipath gains estimation for doubly-selective fading channels," *Phys. Commun.*, vol. 22, pp. 19–31, Mar. 2017.

[6] C. Oestges and B. Clerckx, *MIMO Wireless Communications: From Real-World Propagation to Space-Time Code Design*. New York, NY, USA: Academic, 2010.

[7] M. O. Damen, H. El Gamal, and G. Caire, "On maximum-likelihood detection and the search for the closest lattice point," *IEEE Trans. Inf. Theory*, vol. 49, no. 10, pp. 2389–2402, Oct. 2003.

[8] J. Jaldén and B. Ottersten, "On the complexity of sphere decoding in digital communications," *IEEE Trans. Signal Process.*, vol. 53, no. 4, pp. 1474–1484, Apr. 2005.

[9] C. Windpassinger, L. Lampe, R. F. H. Fischer, and T. Hehn, "A performance study of MIMO detectors," *IEEE Trans. Wireless Commun.*, vol. 5, no. 8, pp. 2004–2008, Aug. 2006.

[10] P. Li, R. C. de Lamare, and R. Fa, "Multiple feedback successive interference cancellation detection for multiuser MIMO systems," *IEEE Trans. Wireless Commun.*, vol. 10, no. 8, pp. 2434–2439, Aug. 2011.

[11] R. C. de Lamare, "Adaptive and iterative multi-branch MMSE decision feedback detection algorithms for multi-antenna systems," *IEEE Trans. Wireless Commun.*, vol. 12, no. 10, pp. 5294–5308, Oct. 2013.

[12] Y.-C. Liang, S. Sun, and C. K. Ho, "Block-iterative generalized decision feedback equalizers for large MIMO systems: Algorithm design and asymptotic performance analysis," *IEEE Trans. Signal Process.*, vol. 54, no. 6, pp. 2035–2048, Jun. 2006.

[13] Y.-C. Liang, G. Pan, and Z. D. Bai, "Asymptotic performance of MMSE receivers for large systems using random matrix theory," *IEEE Trans. Inf. Theory*, vol. 53, no. 11, pp. 4173–4190, Nov. 2007.

[14] Y.-C. Liang, E. Y. Cheu, L. Bai, and G. Pan, "On the relationship between MMSE-SIC and BI-GDFE receivers for large multiple-input multiple-output channels," *IEEE Trans. Signal Process.*, vol. 56, no. 8, pp. 3627–3637, Aug. 2008.

[15] K. V. Vardhan, S. K. Mohammed, A. Chockalingam, and B. S. Rajan, "A low-complexity detector for large MIMO systems and multicarrier CDMA systems," *IEEE J. Sel. Areas Commun.*, vol. 26, no. 3, pp. 473–485, Apr. 2008.

[16] B. Cerato and E. Viterbo, "Hardware implementation of a low-complexity detector for large MIMO," in *Proc. IEEE Int. Symp. Circuits Syst. (ISCAS)*, May 2009, pp. 593–596.

[17] P. Li and R. D. Murch, "Multiple output selection-LAS algorithm in large MIMO systems," *IEEE Commun. Lett.*, vol. 14, no. 5, pp. 399–401, May 2010.

[18] T. Datta, N. Srinidhi, A. Chockalingam, and B. S. Rajan, "Random-restart reactive tabu search algorithm for detection in large-MIMO systems," *IEEE Commun. Lett.*, vol. 14, no. 12, pp. 1107–1109, Dec. 2010.

[19] N. Srinidhi, T. Datta, A. Chockalingam, and B. S. Rajan, "Layered tabu search algorithm for large-MIMO detection and a lower bound on ML performance," *IEEE Trans. Commun.*, vol. 59, no. 11, pp. 2955–2963, Nov. 2011.

[20] P. Som, T. Datta, N. Srinidhi, A. Chockalingam, and B. S. Rajan, "Low-complexity detection in large-dimension MIMO-ISI channels using graphical models," *IEEE J. Sel. Topics Signal Process.*, vol. 5, no. 8, pp. 1497–1511, Dec. 2011.

[21] J. Goldberger and A. Leshem, "MIMO detection for high-order QAM based on a Gaussian tree approximation," *IEEE Trans. Inf. Theory*, vol. 57, no. 8, pp. 4973–4982, Aug. 2011.

[22] T. L. Narasimhan and A. Chockalingam, "Channel hardening-exploiting message passing (CHEMP) receiver in large-scale MIMO systems," *IEEE J. Sel. Topics Signal Process.*, vol. 8, no. 5, pp. 847–860, Oct. 2014.

[23] S. Wu, L. Kuang, Z. Ni, J. Lu, D. Huang, and Q. Guo, "Low-complexity iterative detection for large-scale multiuser MIMO-OFDM systems using approximate message passing," *IEEE J. Sel. Topics Signal Process.*, vol. 8, no. 5, pp. 902–915, May 2014.

[24] T. Datta, N. A. Kumar, A. Chockalingam, and B. S. Rajan, "A novel Monte-Carlo-sampling-based receiver for large-scale uplink multiuser MIMO systems," *IEEE Trans. Veh. Technol.*, vol. 62, no. 7, pp. 3019–3038, Sep. 2013.

[25] Q. Zhou and X. Ma, "Element-based lattice reduction algorithms for large MIMO detection," *IEEE J. Sel. Areas Commun.*, vol. 31, no. 2, pp. 274–286, Feb. 2013.

[26] Z. Luo, M. Zhao, S. Liu, and Y. Liu, "Generalized parallel interference cancellation with near-optimal detection performance," *IEEE Trans. Signal Process.*, vol. 56, no. 1, pp. 304–312, Jan. 2008.

[27] D. Radji and H. Leib, "Interference cancellation based detection for V-BLAST with diversity maximizing channel partition," *IEEE J. Sel. Topics Signal Process.*, vol. 3, no. 6, pp. 1000–1015, Dec. 2009.

[28] D. Radji and H. Leib, "Asymptotic optimal detection for MIMO communication systems employing tree search with incremental channel partition preprocessing," *Trans. Emerg. Telecommun. Technol.*, vol. 24, no. 2, pp. 166–184, 2013.

[29] C. Jing, J. Xiong, X. Wang, J. Wei, and Y. Guo, "Low-complexity group alternate iterative list detection for MIMO systems," *IEEE Access*, vol. 4, pp. 5858–5867, 2016.

[30] L. Ma, K. Dickson, J. McAllister, and J. McCanny, "QR decomposition-based matrix inversion for high performance embedded MIMO receivers," *IEEE Trans. Signal Process.*, vol. 59, no. 4, pp. 1858–1867, Apr. 2011.

[31] S. Moussa, A. M. A. Razik, A. O. Dahmane, and H. Hamam, "FPGA implementation of floating-point complex matrix inversion based on GAUSS-JORDAN elimination," in *Proc. 26th Annu. IEEE Can. Conf. Elect. Comput. Eng. (CCECE)*, May 2013, pp. 1–4.

[32] B. M. Hochwald, T. L. Marzetta, and V. Tarokh, "Multiple-antenna channel hardening and its implications for rate feedback and scheduling," *IEEE Trans. Inf. Theory*, vol. 50, no. 9, pp. 1893–1909, Sep. 2004.

[33] M. Wu, B. Yin, G. Wang, C. Dick, J. R. Cavallaro, and C. Studer, "Large-scale MIMO detection for 3GPP LTE: Algorithms and FPGA implementations," *IEEE J. Sel. Topics Signal Process.*, vol. 8, no. 5, pp. 916–929, Oct. 2014.

[34] H. Prabhu, J. Rodrigues, O. Edfors, and F. Rusek, "Approximative matrix inverse computations for very-large MIMO and applications to linear precoding systems," in *Proc. IEEE Wireless Commun. Netw. Conf. (WCNC)*, Apr. 2013, pp. 2710–2715.

[35] D. Zhu, B. Li, and P. Liang. (Mar. 2015). "On the matrix inversion approximation based on Neumann Series in Massive MIMO systems." [Online]. Available: https://arxiv.org/abs/1503.05241

[36] A. Ben-Israel, "An iterative method for computing the generalized inverse of an arbitrary matrix," *Math. Comput.*, vol. 19, no. 91, pp. 452–455, 1965.

[37] V. Pan and J. Reif, "Efficient parallel solution of linear systems," in *Proc. 17th Annu. ACM Symp. Theory Comput.*, 1985, pp. 143–152.

[38] V. Pan and R. Schreiber, "An improved Newton iteration for the generalized inverse of a matrix, with applications," *SIAM J. Sci. Statist. Comput.*, vol. 12, no. 5, pp. 1109–1130, 1991.

[39] Y. Wang and H. Leib, "Sphere decoding for MIMO systems with Newton iterative matrix inversion," *IEEE Commun. Lett.*, vol. 17, no. 2, pp. 389–392, Feb. 2013.
[40] R. Rosario, F. A. Monteiro, and A. Rodrigues, "Fast matrix inversion updates for massive MIMO detection and precoding," *IEEE Signal Process. Lett.*, vol. 23, no. 1, pp. 75–79, Jan. 2016.
[41] L.-L. Yang, "Using multi-stage MMSE detection to approach optimum error performance in multiantenna MIMO systems," in *Proc. IEEE 70th Veh. Technol. Conf. Fall (VTC-Fall)*, Sep. 2009, pp. 1–5.
[42] A. Chockalingam and B. S. Rajan, *Large MIMO Systems*. Cambridge, U.K.: Cambridge Univ. Press, 2014.
[43] S. Loyka and F. Gagnon, "Performance analysis of the V-BLAST algorithm: An analytical approach," *IEEE Trans. Wireless Commun.*, vol. 3, no. 4, pp. 1326–1337, Jul. 2004.
[44] Y. Jiang, X. Zheng, and J. Li, "Asymptotic performance analysis of V-BLAST," in *Proc. IEEE Global Telecommun. Conf. (GLOBECOM)*, vol. 6, Nov./Dec. 2005, pp. 3882–3886.
[45] V. A. Marčenko and L. A. Pastur, "Distribution of eigenvalues for some sets of random matrices," *Math. USSR-Sbornik*, vol. 1, no. 4, pp. 457–483, 1967.
[46] A. Edelman, "Eigenvalues and condition numbers of random matrices," *SIAM J. Matrix Anal. Appl.*, vol. 9, no. 4, pp. 543–560, 1988.
[47] G. H. Golub and C. F. Van Loan, *Matrix Computations*. Baltimore, MD, USA: The Johns Hopkins Univ. Press, 2012.
[48] T. K. Moon and W. C. Stirling, *Mathematical Methods and Algorithms for Signal Processing*. New York, NY, USA: Prentice-Hall, 2000.
[49] P. W. Wolniansky, G. J. Foschini, G. D. Golden, and R. A. Valenzuela, "V-BLAST: An architecture for realizing very high data rates over the rich-scattering wireless channel," in *Proc. URSI IEEE Int. Symp. Signals, Syst., Electron. (ISSSE)*, Oct. 1998, pp. 295–300.
[50] H. Zhang, H. Dai, Q. Zhou, and B. L. Hughes, "On the diversity order of spatial multiplexing systems with transmit antenna selection: A geometrical approach," *IEEE Trans. Inf. Theory*, vol. 52, no. 12, pp. 5297–5311, Dec. 2006.
[51] A. Paulraj, R. Nabar, and D. Gore, *Introduction to Space-Time Wireless Communications*. Cambridge, U.K.: Cambridge Univ. Press, 2003.
[52] S. Verdu, *Multiuser Detection*. Cambridge, U.K.: Cambridge Univ. Press, 1998.
[53] J. Benesty, Y. Huang, and J. Chen, "A fast recursive algorithm for optimum sequential signal detection in a BLAST system," *IEEE Trans. Signal Process.*, vol. 51, no. 7, pp. 1722–1730, Jul. 2003.

TIANPEI CHEN received the B.Eng. degree in electronic information engineering from the University of Electronic Science and Technology of China, Chengdu, Sichuan, China, in 2013, and the M.Eng. degree in electrical and computer engineering from McGill University, Montreal, QC, Canada, in 2016. From 2014 to 2016, he was a Research Assistant with the Department of Electrical and Computer Engineering, McGill University. Since 2017, he has been with Qualcomm, Inc., where he is working as a Modem System Engineer. His research interests include large-scale MIMO, GPGPU computing, and machine learning.

HARRY LEIB received the B.Sc. *(cum laude)* and M.Sc. degrees in electrical engineering from the Technion–Israel Institute of Technology, Haifa, Israel, in 1977 and 1984, respectively, and the Ph.D. degree in electrical engineering from the University of Toronto, Canada, in 1987.

From 1977 to 1984, he was with the Israel Ministry of Defense, working in communication systems area. After completing his Ph.D. studies, he was with the University of Toronto as a Post-Doctoral Research Associate and as an Assistant Professor. Since 1989, he has been with the Department of Electrical and Computer Engineering, McGill University, Montreal, where he is currently a Full Professor. At McGill, he teaches undergraduate and graduate courses in the communications area, and probability theory. His current research activities are in the areas of digital communications, wireless communication systems, global navigation satellite systems, detection, estimation, and information theory.

Dr. Leib was an Editor of the IEEE TRANSACTIONS ON COMMUNICATIONS 2000–2013, and an Associate Editor of the IEEE TRANSACTIONS ON VEHICULAR TECHNOLOGY 2001–2007. He has been a Guest Co-Editor for special issues of the IEEE JOURNAL ON SELECTED AREAS IN COMMUNICATION on Differential and Noncoherent Wireless Communication 2003–2005, and on Spectrum and Energy Efficient Design of Wireless Communication Networks 2012–2013. Since 2017, he has been the founding Editor-in-Chief of *AIMS Electronics and Electrical Engineering Journal*.